2019-08-01

Development of a Novel Bioprinting System:Bioprinter, Bioink, Characterizationand Optimization

Chandler Alan Warr
Brigham Young University

Development of a Novel Bioprinting System:

Bioprinter, Bioink, Characterization

and Optimization

Chandler Alan Warr

A thesis submitted to the faculty of
Brigham Young University
in partial fulfillment of the requirements for the degree of

Master of Science

Alonzo D. Cook, Chair
Gregory Nordin
Thomas A. Knotts

Department of Chemical Engineering

Brigham Young University

ABSTRACT

Development of a Novel Bioprinting System:
Bioprinter, Bioink, Characterization
and Optimization

Chandler Alan Warr
Department of Chemical Engineering, BYU
Master of Science

The use of 3D printing in biological applications is a new field of study given that 3D printing technology has become more available and user friendly. Possible uses include using existing 3D printing polymers to use in extracorporeal or in vitro devices, like Lab-on-a-Chip, and the development of new biologically derived materials to print cell-containing constructs. The latter concept is what is more commonly known as bioprinting. Our research had the goal of developing a bioprinting system including the printer, a bioink, and a feedback system for printing parameter optimization which could be done cheaply and within the reach of nearly any research lab. To make the bioprinter, we were able to take a popular plastic 3D printer and convert it to a bioprinter with 3D printed parts and the addition of a new motherboard. This came with great contribution from Carnegie Melon University. We were also able to improve upon the original design and, along with the new bioprinting capabilities, maintain the original capabilities of the plastic 3D printer. A new bioink was developed to work in coordination with this bioprinting system. Our lab has the luxury of having access to decellularized tissue, which provided a unique material to create a bioink which is derived from the extra-cellular matrix of porcine hearts. The final bioink protocol allows the users to make their own bioink, from easily obtainable tissue and determine their own concentration of the extra-cellular matrix/collagen within a range. Lastly, a feedback system was developed using a Raspberry Pi and camera module to provide real-time visual feedback of the bioprinting process which is otherwise very difficult to see and optimize parameters from. A protocol was developed to sequentially optimize the parameters for an open-source slicing software which governs the resolution of the bioprinter itself. In related research, the cytotoxicity and cell adherence properties of a printing resin for a microfluidic 3D printer were evaluated for use in Lab-on-a-Chip applications. The existing resin was tested and determined to be cytotoxic to cells and therefore not suitable for biological applications. We showed that a simple ethanol washing step and plasma treatment pulled the cytotoxic elements out of the polymer and modified the surface such that cells could attach and proliferate on the printed resin. Another printed resin was also tested which was determined to have no natural cytotoxicity, but the same plasma treatment was needed to allow for cell adherence.

Keywords: bioprinting, 3dprinting, collagen, tissue engineering, bioink, alginate, cytotoxicity

ACKNOWLEDGMENTS

To my sweetheart, best friend, and wife Collette, thank you for all of your support and for grounding me which helped me more than anything to achieve all I have in life.

I would like to express appreciation to my advisor Dr. Cook for his guidance and help throughout my research and introducing me to the incredible world of tissue engineering.

Thank you to the others on my advisory committee, Dr. Nordin and Dr. Knotts, for all of their feedback and help along the way.

A special thank you to all those who went to bat for me in allowing me to pursue a graduate degree: Dr. Harb, Dr. Fletcher, and others I'm sure I don't know about. Thank you.

A generous thanks to all of my lab members and team mates for their Saturday morning attendance to lab workdays and wonderful contributions.

Many thanks to my funding sources including the BYU Chemical Engineering Department, Gerontology program and graduate mentoring for their contributions without which this research could not have happened.

I could not have done this without support from my parents and family who always knew I could do great things.

Lastly, a big thanks to all of the Chemical Engineering staff and faculty without whom I wouldn't have been able to succeed.

TABLE OF CONTENTS

LIST OF TABLES

LIST OF FIGURES

CHAPTER 1. INTRODUCTION AND BACKGROUND

In the early 1990s researchers from MIT and Harvard keyed the phrase ”Tissue Engineering” as the development of biological substitutes to aid the body in regeneration, which blended the fields of cellular biology and engineering [1]. Since then, tissue engineering has grown and developed with new technologies and applications. Current successes in tissue engineering include MIRODERM from Miromatrix Medical Inc., (Eden Prairie, MN) an acellular wound matrix for surface application, and growth factors for bone regeneration (INFUSE Bone Graft from Medtronic, Minneapolis, MN). Cellular versus acellular and in vivo versus in vitro development of constructs continues to be a topic of research and discussion [2]. Recent discussion in tissue engineering revolves around bioprinting and methods of using this technology to further the field of tissue engineering.

Bioprinting, a derivative of traditional 3D printing, has the capability of quickly producing constructs structurally similar to living tissue that cannot be produced using other manufacturing methods. The development of a bioprinting system capable of reproducing a vascularized tissue could be the answer to the current organ shortage. This thesis will address the development of bioprinting systems to be used in biomedical applications including a novel fused deposition modeling (FDM) style bioprinter and a stereolithography (SLA) bioprinter and resin that have been developed previously. Given the complexity of bioprinting, which includes the printer types, material selection, cross-linking methods, substrate support baths, and print characterization, this introduction will provide a brief background on these topics to give the reader needed context.

1.1 3D Printing

1.1.1 Additive Manufacturing

Three dimensional (3D) printing is a form of additive manufacturing which is the process of progressively adding material to form a desired structure. This contrasts with standard subtractive manufacturing where material is taken away from a bulk to give the desired structure. Subtractive manufacturing is the most common manufacturing method, but it is limited in the designs it can manufacture. Additive manufacturing however, can create much more intricate designs, or designs that are impossible to build through subtractive manufacturing, by building a design up layer by layer. The process of additive manufacturing has become more popular in the form of 3D printing. It is now a fairly simple process to either buy and operate, or make a 3D printer to use at home; it is also becoming a more common manufacturing method in industrial applications. Generally, 3D printing can be broken down into two different categories; DLP/SLA printing (SLA) also known as stereolithography printing and fused-deposition modeling (FDM) printing. Both print using a 3D modeling file operated by slicing software to provide the printer with 2D slices of the model that print layer upon layer. SLA printing consists of an upside-down print bed which is lowered into a liquid resin. The resin is then photo cross-linked with a light source in the pattern desired for that particular layer. FDM printers use essentially a hot-glue gun which extrudes melted plastic into the desired pattern for that layer and is quickly cooled prior to the next layer being printed. SLA printing can reach a resolution of around 20 to 100 μm with harder materials that don't move layer upon layer. FDM printers have a wide range of resolutions that can go down to a motor resolution of about 100 μm using a variety of materials including PLA, ABS, and other thermoset polymers.

Bioprinting is a derivative of traditional 3D printing where the main difference is in the extrusion method. SLA style bioprinters have almost no difference from their traditional counterparts except that material properties will be optimized for biological conditions and cellular contact. FDM style bioprinters have more significant differences from traditional printers of this kind and tend to use a syringe and needle to extrude the paste-like material that is printed. The material properties of this paste, as well as the printer accuracy and needle gauge, help to determine the resolution of the printed constructs. The combined resolution of the printer, needle, and material properties determine what designs can be reliably printed. For instance, if a printer has accuracy

down to 100 μm and a 30-gauge needle is used, which has an internal diameter of 160 μm, then it would be impossible to print a wall 120 μm thick. Even though the motor resolution is below 120 μm, the width of the needle precludes the desired print resolution. The overall resolution of a printed construct is also dependent on material properties; if a material has a high viscosity, it may not be possible to extrude it at the desired rate for printing. Both SLA and FDM style bioprinters have potential for use in biomedical applications if the material properties and resolution can be optimized for biological conditions.

1.1.2 Printing Substrates

FDM-style bioprinters extruding pastes need, in most cases, a substrate support bath to print into since the extruded paste cannot support itself layer upon layer. Imagine trying to print a cube out of toothpaste; the end product would just be a pile of toothpaste in a sort of square. Pastes need to be suspended in a printing substrate while they are liquid and then cross-linked or solidified by various means into their final desired shape. Now imagine printing a toothpaste cube from a needle inside of hair gel. This allows for any shape to be printed, even ones that are not possible by traditional 3D printing, since any given layer being printed doesn't depend on the previous layer printed underneath it for support. One method of doing this is to use a carbomer polymer support gel, similar to hair gel [3] . Another method referred to as Freeform Reversible Embedded Suspension of Hydrogels (FRESH) uses a gelatin slurry, blended to a specified polymer chain length, to create a shear-thinning gel which can be used as a printing substrate. [4] This method is particularly useful in bioprinting because it can be liquified in an incubator at 37 °C from which you can easily remove the printed construct. However, the method of printing within a substrate creates problems not seen in traditional 3D printing. One problem is that of the additional drag created by the printing needle moving through a fluid viscous enough to hold the print material in suspension. This can be helped by tuning the printing substrate to be shear-thinning, but this can't be done with all substrates. Therefore, the printing material and substrate properties need to be optimized together to ensure that the print design can be printed consistently and predictably. There are some materials and methods that don't require a printing substrate, however, these are limited in use currently.

1.1.3 Characterization and Printing Parameters

One of the most difficult aspects of bioprinting is the characterization of the prints, ensuring that the design sent to the printer is actually being produced by the printer. Traditional 3D printing has printing parameters that are optimized using visual feedback. This feedback has been standardized using a benchmark print known as Benchy. This print, which happens to look like a boat, is designed to be difficult to print and provides feedback on the resolution of a particular printer and material combination. This characterization becomes more difficult in extrusion bioprinting because the extrusion must be done within a suspension substrate and visual feedback cannot be relied upon while the print is in suspension. Constructs that have been cured and pulled out of suspension can give feedback for printing parameters, but it is possible that the curing process could swell or shrink the construct and provide false data. These data are needed in order to optimize printing parameters such as extrusion width and height, overlap, and extrusion multiplier. The inability to optimize these parameters to the micron level is a problem yet to be addressed in detail and will be discussed in Chapter 4.

1.2 Material Characteristics

1.2.1 Material Options

SLA printing technology currently works with many different materials and photoinitiators, generally using polymer resins which can mimic the feel of materials such as polypropylene, clear polycarbonate, and rubber. SLA printer materials are generally limited by the photoinitiated curing method but must also have a low viscosity such that the print platform can be quickly cleared of uncured resin. The types of materials used in SLA printing may be very useful for biomedical devices, both implantable and extracorporeal, but may not be as useful for cell-laden tissue scaffolds. On the other hand, FDM bioprinter materials range from native bioinks like collagen and fibrin, to alginate and other hydrogels, and even silicon rubber. These materials can be cross-linked using multiple methods including photo, catalytic, chemical, and thermal cross-linking depending on the material. This gives flexibility to the material selection since materials can be mixed at different ratios and optimized for various applications. However, one necessary property of these extruded materials is that they are thin enough to be extruded through a needle small enough to maintain

good print resolution. This means that high-viscosity materials require a larger needle which results in a lower resolution. If higher resolutions are desired, smaller needles or a shear-thinning material must be used.

1.2.2 Biocompatibility

A final property to consider regarding bioprinting materials is that of biocompatibility. Biocompatibility needs will differ depending on the purpose of the printed construct; whether it is an acellular extracorporeal device, an acellular implanted device, or intended as a cell-laden tissue scaffold. Overall, bioprinted constructs need to be nontoxic to cells, which may require post-print processing, and not have an inherent immune response when implanted. Additionally, since almost all bioprinted constructs will be blood contacting, they need to have non-thrombogenic properties that will minimize clotting within the construct. Non-thrombogenic properties can, however, be introduced during post-processing with surface modifications, such as a heparin coating, if they are not inherent within the material. Lastly, if the intent of the construct is for tissue generation, then the use of native materials, materials such as collagen and fibrin which are naturally occurring in the body, becomes increasingly important as those will likely be more easily remodeled by inlaid cells.

CHAPTER 2. BIOPRINTER MECHANICAL AND ELECTRICAL MODIFICATION

2.1 Background

2.1.1 Additive Manufacturing

Many different methods of additive manufacturing are available to researchers worldwide to investigate possible applications within tissue engineering. These include electrospinning, lamination, and various methods of 3D printing as researchers have looked into methods to manufacture an in vivo vasculature [5, 6]. Bioprinting has sparked recent interest because of its ability to build complex structures and the variety of usable materials that are available. Various methods of bioprinting have been examined in detail by many different researchers in evaluating printing methods with their associated resolution and advantages [7–9]. Generally, SLA and FDM style bioprinters are most common and seem to have the highest probability of producing viable tissues and extracorporeal/implantable devices.

SLA bioprinting uses the same methods and machinery as traditional 3D SLA printing but differs in the application of printed constructs. SLA printed constructs have application in tissue engineering as extracorporeal or implantable acellular devices. Given the resins are cured via UV light in most cases, this precludes the use of cells within the constructs themselves since this curing method would kill inlaid cells. There are resins under development that use light in the visible spectrum to cure, however the use of cells in these printers is unlikely because of the nature of the printing process and the non-native properties of the resins [10]. Several researchers have printed porous scaffolds upon which cells were seeded to create cell-laden constructs [11,12]. Additionally, researchers at BYU have developed a printer that can reach a resolution of 20 μm in a channel width which approaches the inner diameter of a capillary bed [13]. Other researchers have taken this same idea and made similar transparent devices that have cultured cells for several days after washing [14].

FDM bioprinters have become popular because of their similarity to traditional 3D extrusion printing and the gentle nature of cross-linking conditions that exist. As noted in the introduction, FDM bioprinters consist of a needle and syringe and the resolution of these printers is dependent upon many factors including the step resolution of the motors, the needle size, and material properties. The step resolution of a printer will be defined by the manufacturer and depends on the motors used and the gearing ratios for each axis. Generally, there is a trade off between step resolution and print speed, meaning that very high-resolution printers take much longer to print. The needle size is key in print resolution and of particular interest because in cell-laden constructs, cells will have to survive the journey from the syringe, through the needle, and into the construct. Studies have been done on the relationship between the needle diameter and the associated shear-stress on the extruded ink and cells showing that a parameter optimization index (POI) may be helpful in optimizing the needle size, print speed, and pressure [15]. This is an area where more research needs to be done in order to verify, at the micron level, that the print designs going into the printer are coming out of the printer and verify the printing parameters. This could be done by extruding a polymer-like material that would be easier to measure and allow for the iteration and optimization of printing parameters. Thus far, no method has been shown to characterize prints beyond visual confirmation.

Several different FDM extrusion printers have been developed by researchers including the ITOP system and an MIT printer as well as industry made printers including Allevi printers, Cellink printers, and the Matrix printer. The ITOP system was developed at the Wake Forest Institute of Regenerative Medicine and has been shown to print reliable anatomically-correct prints [16]. MIT researchers have used another in-house printer to develop thick vascularized constructs with inlaid cells which have proven successful [17]. The biomedical industry has produced several printers with proven capabilities in printing a variety of materials. These printers span from $10,000 to over $200,000 for industrial bioprinters and generally have a motor step size resolution of around 1 μm. However, it is becoming more popular to modify traditional 3D desktop printers to allow for syringe extrusion and further adapt them for various cross-linking needs that may come about depending on the bioink used.

2.2 FlashForge Creator Pro and Duet WiFi Motherboard

The Tissue Engineering Lab at Brigham Young University had a Seraph Robotics Fab@Home Dual Extruder which originally cost $4488 when it was purchased in 2016 shown in Figure 2.1. This bioprinter worked on hardware and software that predated the 3D printing revolution which standardized the types of stepper motors used in 3D printers as well as the code that these printers and CNC machines run on, known as gcode. This meant that older software needed to be used in conjunction with the printer that did not take advantage of the vast array of open-source software that is available for newer 3D printers and with commercially available bioprinters. We determined that it would be helpful to obtain a new bioprinter that would be much more user friendly and able to achieve the resolution that would be required for the bioprinting applications we had in mind.

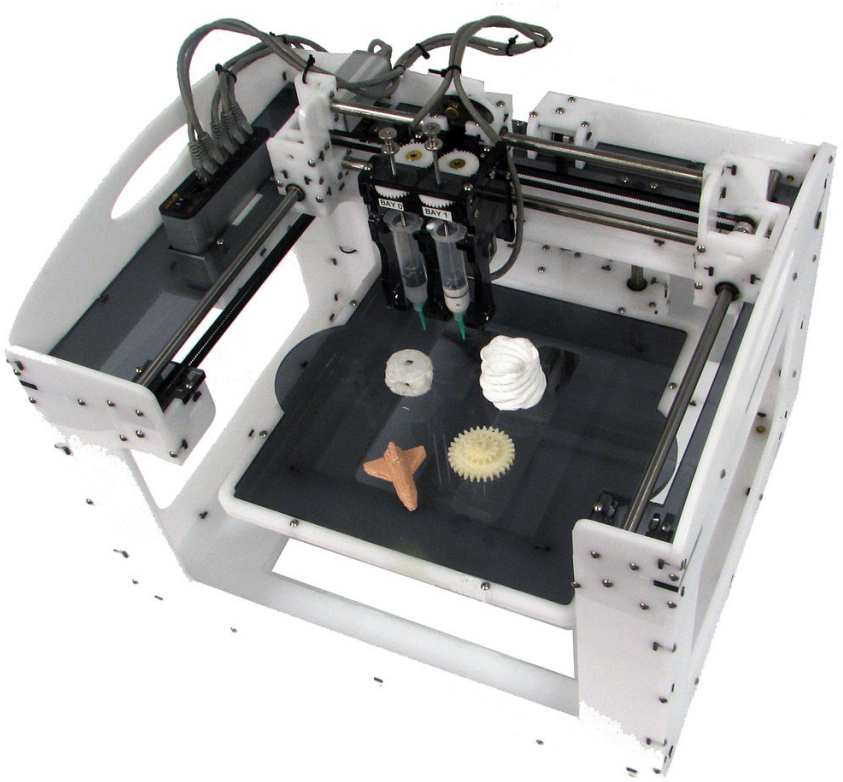

Figure 2.1: Seraph Robotics Fab@Home Dual Extruder

The search for a new bioprinter began by evaluating models from Allevi, then Biobot, and CELLINK. These were priced within the $5k - $10k price range, which is reasonable in the small

niche world of bioprinting. However, this was outside of the budget our lab had at the time and we continued to look into other options. In the meantime, we were looking into bioinks to use in conjuction with these bioprinters and were approached by a company out of Santa Clara, California. Advanced BioMatrix is a leading distributor of research-grade collagen with ties to Brigham Young University and they were in the market to develop several bioink lines to sell to bioprinting researchers. With their help we were able to make some connections to both Biobot to get a beta-test version of their printer as well as T.J. Hinton at Carnegie Mellon University who was making DYI bioprinters accessible to researchers. The Biobot beta-testing printer did not pan out, but the connection with Carnegie Mellon University brought the possibility of making our own bioprinter at a much cheaper price than what we could otherwise do. Subsequent discussions with T.J. Hinton revealed that this would be a wonderful opportunity to get a high-resolution bioprinter into the lab at the cheapest possible price. T.J. Hinton had developed a method to modify a printer popular among 3D printing hobbyists for its ability to be easily modified. This printer, the FlashForge Creator Pro shown in Figure 2.2, cost around $1000 and has an X/Y axis resolution of 100 μm. T.J. had the goal of selling the instructions to do the modification of this 3D printer into a bioprinter for a profit, but the instructions were still being worked on. We agreed that he would share the instructions with me in their current state if I would give him feedback on how to improve them from a consumer standpoint. At that point it was time to buy the printer and start the modification.

As mentioned above, the FlashForge Creator Pro 3D printer was purchased for around $1000 along with a Duet WiFi motherboard to work with the new extruder system that we would be building for the bioprinter. The existing motherboard on the printer ran on its own firmware and wasn't able to be easily modified for the bioprinter; specifically, the motor steps/mm parameter was going to be drastically different from the original printer as we were converting a traditional 3D printing plastic-melting hot-end to a syringe based extrusion system. According to T.J.'s design, the existing motherboard in the printer was to be switched out and all of the wiring moved over onto the new Duet WiFi board. However, while the process of getting the parts for the printer was happening, we found that the plastic 3D printer itself was very useful in the lab and we didn't want to lose that functionality if at all possible. We therefore decided to try and find a way to keep both motherboards mounted and be able to switch between the two when we wanted to do either plastic 3D printing or bioprinting. To solve this problem we came up with a solution involving a

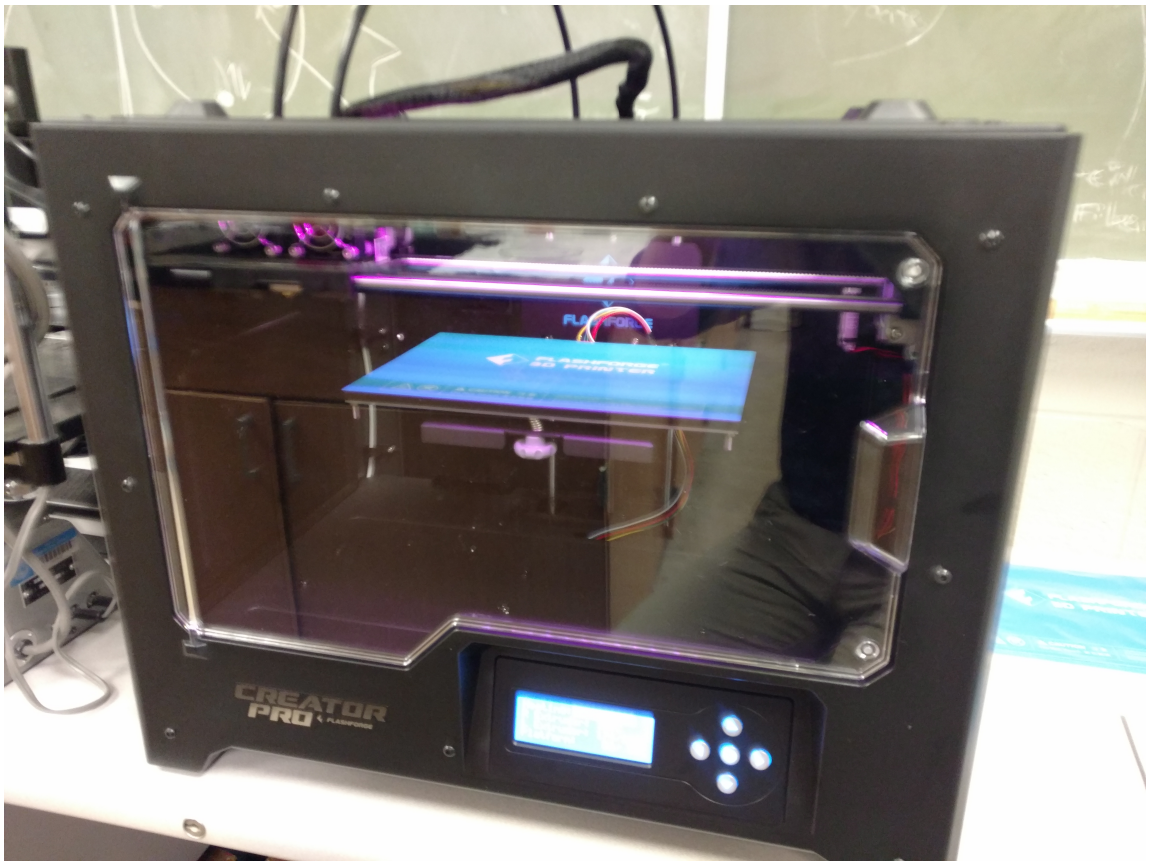

Figure 2.2: FlashForge Creator Pro 3D printer before modifications

large switch array that would switch the signal wires going to the motors from one board to the other as well as the power supply to each board. As seen in Figure 2.3, this was done by using the common wire as the input to each of the motors (of which there are four for each of the three axis-motors) and then attaching the other two terminals to each of the outputs from the two different boards. This had to be done while ensuring that the directionality was consistent between all of the switches when they were mounted so that it was clear for the user as to which motherboard was in play at any given time. The power supply was treated in a similar manner with the inlet coming into the common terminal and the outlet being attached to the toggle switch which could switch between and power the two boards separately. This switch also included a center-off function so that it could be used as a power switch as well if necessary. The switch array example wiring is seen in Figure 2.3B-C. With the wiring finished and tested we could now move to the programming of the firmware for the new motherboard. Each of the axes stepper motors needed to have set in the firmware the conversion between how many steps the motor takes and how that translated into

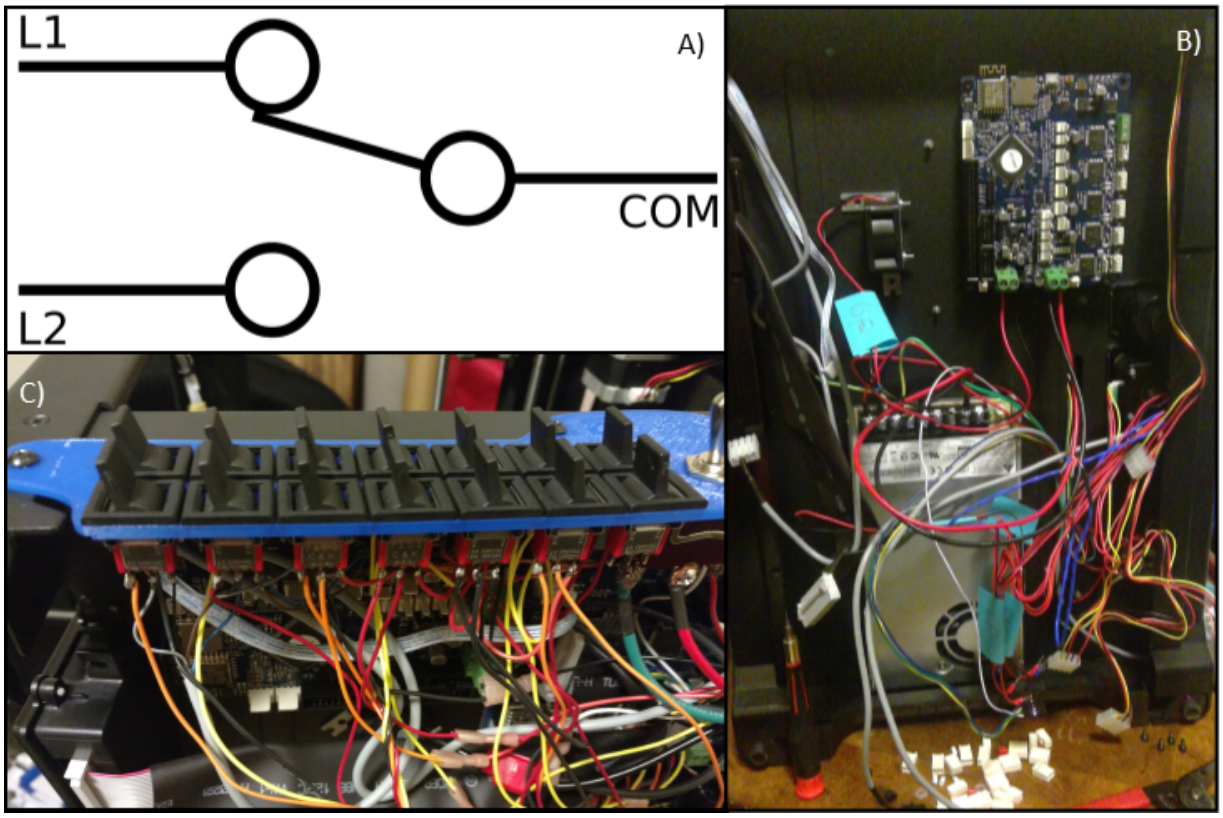

Figure 2.3: FlashForge Creator Pro printer modifications A) SPDT wiring of switch array B) Example of the motherboard modifications C) Switchboard array to switch power supply and motor signals from one board to the other.

a distance that the extruder or printing bed is moved. This is known as a steps/mm parameter and for each of the axes that parameter didn't change so it could be copied over from the firmware of the original motherboard without difficulty. However, the extruder on the bioprinter is entirely different from the 3D printer and this parameter had to be experimentally determined after the extruder was constructed which will be discussed later. With these modifications the FlashForge Creator Pro was finished with the electrical and mechanical modifications and the extruder itself needed to be constructed.

Long after our modification of the FlashForge Creator Pro to our own in-house bioprinter, I was contacted by Advanced BioMatrix, the company that originally connected us with T.J. Hinton, about beta-testing a printer for a start-up company they were working with. This company, SE3D, had received an SBIR grant and were making cheaper bioprinters for use in research and as educational tools in secondary educational settings. After talking with them we received one

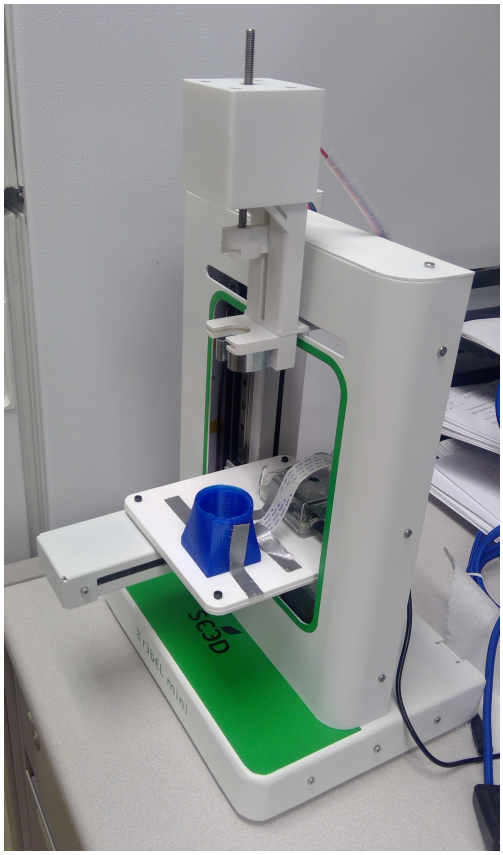

Figure 2.4: SE3D Matrix Bioprinter

of their bioprinters called the MatrixBioprinter, seen in Figure 2.4. It runs on the same Duet WiFi motherboard we installed on the modified printer, but uses a slightly different type of extruder. The original modified FlashForge bioprinter used a gearing system to transfer rotational motion produced by the stepper motor to a linear motion to push a syringe up and down. This worked fine, but had a lot of slack in the system and losses that created a lot of friction between the stepper motor and the plunger. The SE3D extruder used a direct system where the stepper motor had a linear actuator that extended through the motor itself and allowed for much finer control of the syringe without all of the losses. This printer was used often in our research because it was smaller and much easier to carry around versus the FlashForge bioprinter.

2.3 Paste Extruder Design and Construction

With the modification made to the FlashForge Creator Pro which maintained the plastic 3D printing abilities, it was time to turn to the construction of the extruder system. The system

used on the FlashForge bioprinter was designed by T.J. Hinton and represents the bulk of his contribution to the conversion. The hot-end plastic extruder on the original FlashForge Creator Pro was completely replaced by a 3D printed version which allowed for a variety of sizes of glass syringes to be attached and held firmly in place while the plunger was moved by the extruder motor, resulting in a predicable extrusion from the end of the syringe. As partially seen in Figure 2.5, the extruder consists of a rail carriage able to fit three extruders, and the extruder-motor component itself. The extruder-motor component contained a main body to hold the bulk of the syringe, a gearing system, motor mounting attachment, and syringe securement mechanism. All of these parts were 3D printed in PLA, and attached together with hex screws and nuts.

This particular design was developed early on by T.J. Hinton and his team at Carnegie Mellon, and there are flaws that we tried to address while using it. Carnegie Mellon is currently working on a newer version and have changed the design to include a tube attaching the extruder syringe end and the needle tip in a sort of "Bowden-style" design. We have not tried this version in the lab, but slightly modified the original extruder to help its usability. The original extruder was designed to use glass syringes but many times a plastic syringe was easier to use over a glass one. We designed a small plastic insert that would allow plastic syringes to be used which made it more practical for lab use. However, the extruder still had a lot of slack and play in the gearing system and plunger versus the direct drive system seen on the SE3D extruder.

2.4 Summary

With the end goal of tissue engineering being the construction of human tissue, the process of additive manufacturing seems to be one of most broadly used methods to get there. Bioprinting uses additive manufacturing to lay down biologically compatible materials, possibly laden with cells, to build a tissue-like construct that can then mature and be implanted. With the help of Advanced Biomatrix, SE3D, and T.J. Hinton from Carnegie Mellon University, we were able to get two bioprinters into the lab. The first printer was modified from a FlashForge Creator Pro 3D printer with a 3D printed extruder. During this process we made additional modifications along the way including a switch array that allows the printer to have dual functionality as a 3D printer and a bioprinter. The extruder was printed using the plastic 3D printing function on the printer and allowed the plastic hot-end of the extruder to be replaced by a paste-extruder which used a glass

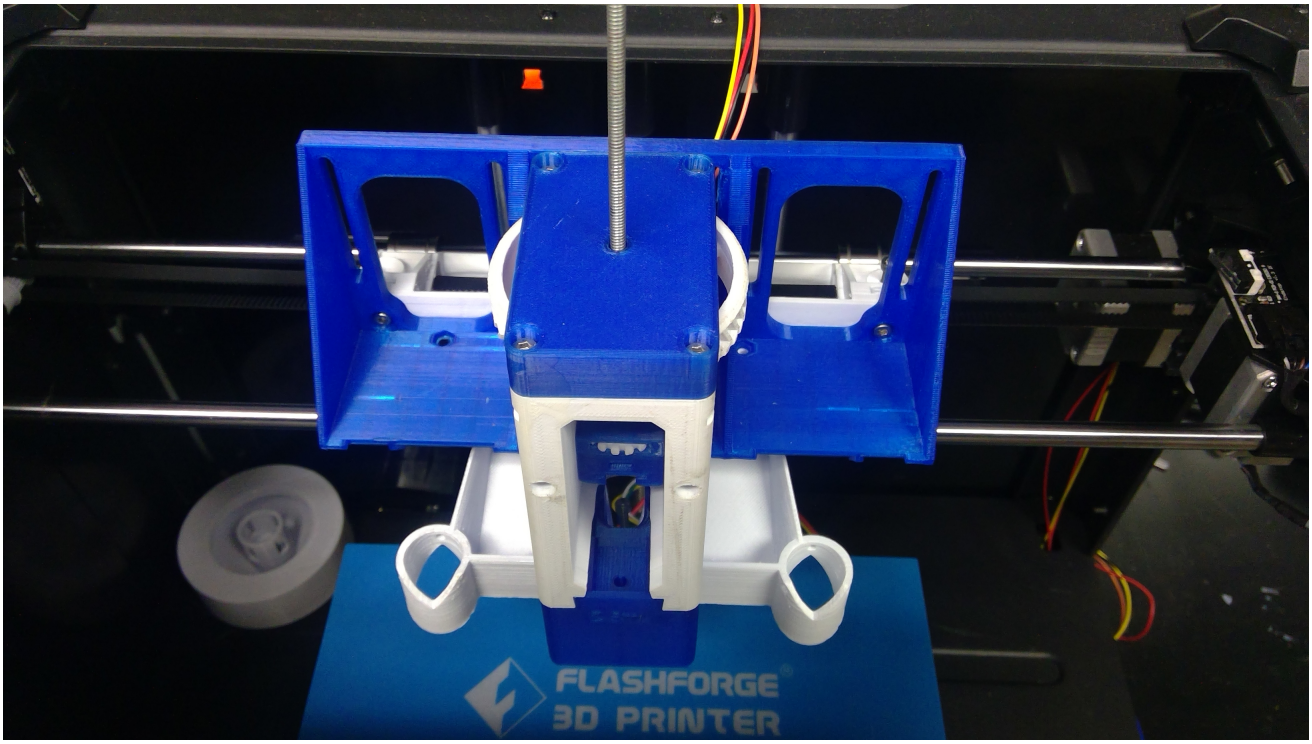

Figure 2.5: 3D printed extruder mounted to the modified FlashForge Creator Pro bioprinter. Has spots for three extruders.

syringe. After the completion of the printer conversion we were also able to obtain a beta-test version of SE3D's Matrix Bioprinter which was used in the lab extensively. The extruder on the SE3D printer had features including a direct-drive system which could more accurately control the syringe plunger versus the converted FlashForge printer. This part of the project concluded with two working bioprinters in the lab as well as a plastic 3D printer that can perform the dual functionality of the FlashForge bioprinter.

CHAPTER 3. BIOINK FORMULATION AND TISSUEBOX DESIGN

3.1 Background

3.1.1 Material Characteristics

Printing materials become important for FDM and SLA style printers with complex constraints such as biocompatibility and cross-linking methods. FDM material selection and development is currently a popular area of publication, and many articles have appeared in the last year addressing a variety of materials. Many researchers have performed detailed reviews into available materials as well as potential needs for future material development in FDM bioprinting. Researchers in Germany recently discussed the bioprinting of structural proteins and their eventual use in the formation of an extracellular matrix scaffold [9]. In the area of bioprinting hydrogels specifically, many researchers are looking into using hydrogel blends such as collagen-alginate, collagen-methacrylated gelatin, alginate-polyvinyl alcohol, gelatin-alginate, and others, which have varying levels of success when it comes to printability and biocompatibility [18–22]. Most popular currently is a collagen bioink sold by Advanced BioMatrix as Lifeink 200, a pure Type 1 Collagen bioink (https://www.advancedbiomatrix.com/bioinks-for-3d-bioprinting/lifeink-200-concentrated-type-i-collagen-5202-1ea/). This bioink is, however, expensive for labs with limited funding and not customizable in terms of the collagen concentration. Some research has been done in deriving a collagen-based bioink from the extra-cellular matrix of decellularized organs (dECM) which holds promise for a cheaper but still native-like bioink [23,24]. There remains, however, a need to more fully develop these decellularized bioinks. A practical approach to making and tailoring them in the lab would provide a collagen bioink source for researchers to use for their own needs.

3.1.2 Printing Substrates

Paste-extruding FDM style bioprinters need to print in a support substrate to suspend bioinks prior to cross-linking. This printing substrate needs to be viscous enough to hold the bioink in suspension but thin enough to allow for needle movement and not affect the surrounding deposited ink. Researchers from Carnegie Mellon University have developed two different methods of doing this, using a carbomer polymer gel and a blended gelatin bath. The carbomer bath has been shown to be useful in printing poly-dimethyl siloxane, a silicone polymer, and other non-biological material [3]. Another method referred to as freeform reversible embedded suspension of hydrogels (FRESH) is used with collagen and other more delicate and thermally cross-linked bioinks [4]. These two printing substrates cover most needs related to bioprinting, though there are a number of other possible products that have similar properties that could work as substitutes.

Some printing methods, known as scaffold-free, don't require the use of a printing substrate because either the ink used is sturdy and stable enough to support itself layer upon layer, or the print method allows for other means of support. One method shown by researchers used cell-laden cylindrical agarose rods stacked up into desired designs to assemble a simple vasculature [25]. Thyroid organoids were developed in another study where a collagen gel held cellular spheroids which gradually grew together to form functional thyroid tissue [26]. UV cross-linkable hydrogel inks have also been shown to be extruded without a support substrate depending on when in the printing process curing occurs [27]. In developing an artificial urethra, researchers have shown that a cell-laden blend of PCL/PLCL is structurally sound enough to be printed on its own and provides a framework upon which urothelial and smooth muscle cells can grow and mature [28]. These scaffold-free printing methods provide promise, however they are difficult to use with biologically native materials currently in use.

3.2 Freeform Reversible Embedded Suspension of Hydrogels - FRESH

During bioprinting, paste-like extrusions are held within a syringe and dispensed through a needle to await cross-linking where they become more solid-like. Maintaining the printed shape while the cross-linking happens, by whatever mechanism that may be, is one of the unique problems of bioprinting. An excellent way to overcome this problem is to print into a substrate with a

tunable viscosity such that it will hold the printed bioink in place until it is cross-linked and then release it by dropping the viscosity. Normal plastic 3D printers print in air as a substrate which works well for the thermal cross-linking that takes place, but air is not practical for bioprinting. Researchers at Carnegie Mellon University developed a method call the Freeform Reversible Embedded Suspension of Hydrogels, called the FRESH printing method for short, which takes gelatin which has been gelled and cuts it into small particles which acts like a viscous slurry similar to the consistency of hair gel as seen in Figure 3.1. This gelatin slurry is thick enough to hold bioinks in place while they are printed and has the unique property of being shear-thinning. This is advantageous in bioprinting because the needle is traveling through this printing substrate during the printing process and if the gel is shear-thinning then the momentum transfer of the needle as it is moving won't disturb previously extruded materials and ruin the resolution of the print. The FRESH gelatin slurry can then be heated after the bioink is cross-linked and the gelatin will melt, greatly reducing its viscosity and the print can be released from the printing substrate. The melting occurs under 37 °C which is physiological temperature and the temperature at which cells are incubated, so the releasing procedure doesn't harm inlaid cells. This melting property, the shear-thinning properties, and the inherent biological compatibility of gelatin combine to make the FRESH printing method very popular and ideal for thermally cross-linking bioinks like collagen that will be discussed later.

3.2.1 Protocol

This method of printing was laid out in a journal article along with the protocol to make it [4]. When we first came across the paper and protocol it was apparent that this was the method that would work well for our purposes. Initial tests showed that making the FRESH was quite difficult and not a simple procedure to master. During this process I was able to visit Advanced BioMatrix in San Diego, California, the company that makes the Lifeink line of bioinks, to see their plant and discuss a possible collaboration and SBIR grant. While there I was shown how they made the FRESH gelatin-slurry and saw a few things we could improve upon in our protocol and were able to obtain a copy of their protocol in the process. The protocol that follows is a compilation of the original protocol published by Carnegie Mellon University, the protocol provided by Advanced Biomatrix, and our own modifications to make the gelatin-slurry with our equipment.

Figure 3.1: Gelatin slurry used in Freeform Reversible Embedded Suspension of Hydrogels (FRESH) printing

FRESH Protocol

Accessories:

1. Gelatin (Type A 150-300 Bloom)
2. Distilled water
3. Stirring hot plate
4. Spatula
5. Blender with individual serving cup attachment
6. Glass beaker

Protocol: Part 1: Preparing the Gelatin

1. Introduce 250 mL of distilled water and 10 g of gelatin to 500mL glass beaker.

2. Mix solution on a hot plate with a fast stir bar, with hot plate at 150 °C until gelatin dissolves. Fully dissolved solution should be transparent. With the stir bar going fast, little bubbles will exist in the solution while on the hot plate. These will disappear, and the solution will become transparent shortly after removing the beaker from the hot plate.

3. Pour solution into individual serving cup from the blender. Wash beaker and stir bar.

4. Store in refrigerator until set (10 hours is plenty).

Part 2: Blending gelatin

*Having cold water will help prevent gelatin from melting into solution when doing multiple washes.

1. Remove mason jar from the refrigerator and fill the remaining space halfway with cold water.

2. Take a spatula and separate the gelatin from the walls of the jar to introduce water between the sides (not the bottom) of the gelatin puck and the container (Ensure full separation of gel from the sides, or the gelatin will not blend correctly).

3. Fill the jar in the sink with additional cold water. Get a big meniscus over the lid.

4. With the jar still in the sink, carefully screw the blender blade lid on the jar. Water will pour out, but you should have avoided introducing much air into the jar. Only a tiny air bubble should be present now. If a substantial air bubble exists more washings will be required later: Take lid off, fill with more water, and repeat.

5. Place the jar (with the attached lid/blade) into a -20 °C freezer for 2-5 minutes. This will help to prevent the gelatin from melting during blending.

6. Blend mixture by holding down the jar for 20 seconds. Make sure that gelatin puck drops within the first 5 seconds on the first blend.

7. Place the blender in the freezer for approximately 1 minute.

8. Repeat steps 6. and 7. six more times, so the total blending time is 140 s.

   *Avoid adding unnecessary heat to the system by not holding the jar with your entire hand.

   *If blender overheats, the gelatin will turn into a big clump. Keep it cold.

   *After blending, the solution should be pipettable and not overly viscous/gelatinous.

   *Keep all materials cold (refrigerated) from this point forward as warming the solution will cause the gelatin particles to melt.

Part 3: Centrifugation

1. Pipette 45 mL of the gelatin slurry into 50 mL centrifuge tubes.

2. Centrifuge at 3,800G for 2 minutes at 4 °C.

   After centrifugation, the tube should contain a compacted pellet of gelatin slurry with a somewhat cloudy supernatant, and a white foamy top layer. This white foam raft is the soluble gelatin. (Ideally, the white foamy layer is minimal or non-existent.)

3. Pour off the supernatant and raft (if there). If there was no foamy raft, you are done; store the FRESH slurry in an airtight container. If there was a foamy raft:

   (a) Refill tube with cold water.

   (b) Shake vigorously or vortex to re-suspend all the slurry. Shaking vigorously helps introduce air bubbles, which help in removing soluble gelatin. It is fully suspended when there is no more slurry at the bottom of the tube.

   (c) Repeat steps 2 and 3 until no to little foam is observed at the top of the supernatant. This indicates that most of the soluble gelatin has been removed.

   (d) After the last centrifuge, the slurry is ready to use. If storing, refill the tube with cold water and mix again. Store the FRESH slurry in a refrigerated airtight container.

This protocol is different from others in the blending method. The original protocols took the gelatin puck and did the entire blending in a single step. This took up to 90 seconds of blend time and had the risk of overheating and destroying the blender itself. At times the blender itself

was put in the freezer before and during the blending of the gelatin to try to avoid this issue when doing the blending in a single step. After some experimentation, we found that a series of shorter blending times gave us the same result as a single long blend without the risk of overheating and ruining our blender.

This method of making the FRESH worked very well for us and produced very consistent results that we could use as a printing substrate. Though our work never progressed to the stage to where we printed with live cells, it was still necessary to find a way to sterilize the FRESH in preparation for that. In general, sterilization techniques include chemical, radiation, and thermal. After the gelatin slurry was made, it clearly could not be sterilized thermally in an autoclave as it would destroy the gelled structure of the particles that had been created. Chemical sterilization was attempted using 70% ethanol, but an esterification reaction resulted in a gelling of the slurry which destroyed the micro-particles that were formed during the blending process. After a discussion with T.J. Hinton at Carnegie Mellon University, we decided to try and sterilize the FRESH from the beginning of the process and sterilized the powdered gelatin via UV radiation from a 30 minute exposure to the UV sterilizing light in our biosafety cabinet, as a part of it's normal sterilization procedure. Then sterile water and other sterile materials were used throughout the rest of the process of making the slurry. This proved to be difficult, with lots of places to make an easy error, but in the end we were able to make sterile FRESH using this method.

3.3 Alginate

The first material that we used as a bioink was alginate, a polysaccharide derived from brown seaweed. Alginate is commercially used as a thickening agent in food and drinks and is the gel-like shell of popping boba and fake caviar. In tissue engineering research, alginate is used as a hydrogel for cell encapsulation, wound healing, and drug delivery. It has excellent biocompatibility, a very low toxicity when interacting with cells and can be cross-linked gently for cell encapsulation [29].

Alginate is generally found as a salt in coordination with sodium and is bought as a powder. This powder is dissolved in water while stirring to achieve different concentrations. The alginate powder generally has a hard time forming a homogenous mixture and requires continuous stirring to make a good gel. The higher the concentration of alginate in the water the more difficult the

mixing becomes. Common concentrations are around 0.1% - 5% by weight. Alginates will have a wide variety of viscosities based on their concentration and do show some shear-thinning behavior. At low shear (0.01 s^{-1}) the viscosities can vary from 1 - 1000 Pa s^{-1} for various concentrations and molecular weight [30]. Because bioprinting uses a needle, usually around 100 - 500 μm in inner diameter, this viscosity and the extent of the shear-thinning behavior strongly impact the use of alginate in bioprinting. Alginate gels that are too thick simply can't be extruded through the needles with the pressure generated by the stepper motor when pushing on the plunger. The cross-linking method also impacts how alginate is used in bioprinting. Generally, sodium alginate is cross-linked by calcium ions which ionically cross-link alginate strands and form the hydrogel. This would be under the category of chemical cross-linking and and presents a unique challenge when bioprinting is popularly done in a printing substrate such as FRESH as previously discussed. The challenge is that calcium needs to be introduced into a gelatin slurry substrate after the alginate has been extruded. It has been found that mixing a low concentration of calcium chloride into the printing substrate will allow the alginate to be slowly cross-linked as it is extruded but allow time for parallel extrusions to gel together and not as individual strands as demonstrated in Reference [4].

Alginate is often used as a bioink on its own or as a component of a complex bioink. Alginate has been used as a general purpose bioink mixed with gelatin [31], in 3D cell culture [32] [30], and in bone tissue engineering in conjunction with polyvinyl alcohol and hydroxyapatite [33]. Alginate was used as the first real bioink in our research and was used extensively for several months. Generally a 2% alginate concentration was used in the bioink and an 11mM $CaCl_2$ was incorporated in the FRESH printing substrate. This created an alginate shell that would slowly cross-link in the FRESH solution, but we found that it was necessary to add more calcium to the alginate to sufficiently cross-link it so that it could be handled. This was done by sprinkling $CaCl_2$ pellets on the top of the container holding the FRESH and printed alginate. There was enough water in the FRESH slurry that the $CaCl_2$ was quickly dissolved and helped to further cross-link the alginate. In initial investigations, we were simply trying to find the practical limits of resolution on the alginate bioink in a FRESH substrate. A 16-gauge needle was used to start which gives a large inner diameter of 1.19 mm. This clearly decreases the resolution of a particular print because the larger cross-section of the extrusion from the needle means you have thicker layers and overall fewer extrusion passes to create the structure. Figure 3.2 shows an example of what was printed

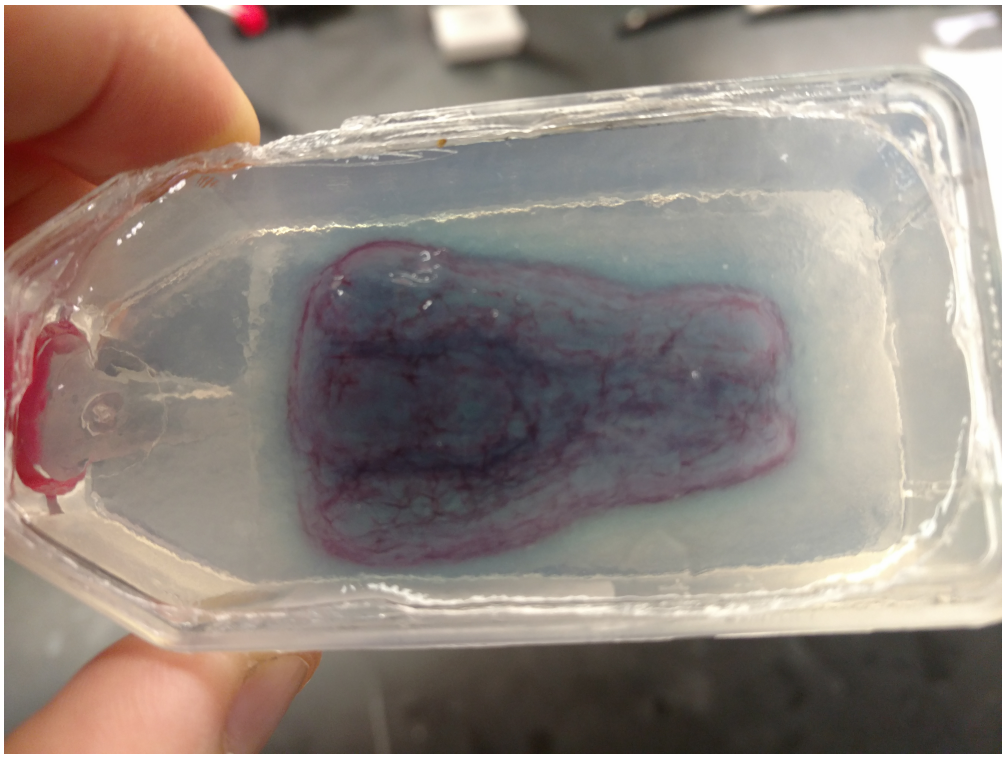

Figure 3.2: Bioprinted alginate showing a bifurcated channel. Resolution is poor and the channels were not as open as originally printed becuase of the swelling nature of the cross linked hydrogel.

using this thicker gauge needle. The resolution was poor and it was difficult to achieve consistent results. One problem that became apparent was the fact that alginate swells as it is cross-linked, and that swelling ratio changes depending on the alginate concentration. This is one of the reasons that we started to look into other bioinks or blends that would provide properites that could be tuned to our needs.

3.4 Decellularized Collagen-Based Bioink

Collagens are the most abundant protein in the body and are a major structural component of all tissues. Tissue consists generally of cells, the functional unit in biology, and the extracellular matrix (ECM), which exists between the cells and provides structural and nutritional support. The major protein in the ECM is collagen, a structural protein made from a repeating three amino acid sequence consisting primarily of glycine and proline residues in a triple helix structure. Collagen can be derived and purified from many sources including bovine, rat, porcine, and human. Purified and dissolved collagen can have the rheology modified depending on the concentration and

temperature of the collagen, as well as the type [34]. Uncross-linked collagen can be cross-linked back to a native-like state by thermal and chemical means depending on the application [35]. Traditionally, a thermal mechanism is used which only requires the temperature to be raised to 37 °C, the temperature at which cells are incubated, which makes thermal cross-linking very handy.

Collagen is used in tissue engineering research as 3D porous constructs, gels, wound healing constructs, and many other applications. Collagen, such as the types sold by Advanced BioMatrix (https://www.advancedbiomatrix.com), can be used in similar applications where Matrigel would be used in making gels and encapulating cells. Recently there has been a huge increase in the use of collagen in bioprinting applications as this manufacturing method has taken off in the tissue engineering world. To only list a few, researchers around the world are using collagen in the following bioprinting applications.

- Bioprinting a cornea replacement for implantation [36]
- Developing a blood vessel network for tissue generation [37]
- Tissue engineering applications for artificial blood vessels [38]
- Bioprinting a tracheal segment in a rabbit study [39]
- Bioprinting a hybrid cardiac patch for myocardial repairs [40]
- Heart valve replacements bioprinted from collagen and elastin [41]
- Recreating a liver microenvironment with a collagen hyaluronan bioink [42]

All of these examples use collagen and several use a specific bioink developed by Advanced BioMatrix called Lifeink 200. This is a concentrated Type 1 collagen that has been modified to be stable at room temperature and not begin to cross-link until 37 °C. This is advantageous over other collagens that will start to cross-link at room temperature even though they don't fully cross-link until they are placed in an incubator at 37 °C. With Lifeink 200, bioprinters don't need to be kept in a low-temperature environment while printing: it can simply be done at room temperature. One downside to Lifeink 200 is the cost at $230/5 mL. Although this is not an exorbitant amount, for labs with little funding this cost adds up quickly, particularly if you are printing anything

of substance around the 1 mL range. Another problem is that you are not able to specify the collagen concentration. When printing straight collagen this may not be a concern as the provided concentration works well for many applications, but when blending different materials together to form a new bioink, changing the collagen concentration can be very helpful. To address these concerns and alleviate the cost of the bioink, we decided to make our own bioink as other labs have done which would provide us a consistent supply of our own custom made bioink.

The purification of collagen required expertise and equipment that we did not possess, we therefore went with a slightly more unconventional bioink that we did have the ability to manufacture. We decided to go with a bioink slightly different from Lifeink 200 in the form of a decellularized ECM (dECM) bioink. In its nature, a dECM bioink is composed of mainly collagen, as the ECM itself is mostly collagen, with other additives that were a part of the ECM in the particular region where the tissue was harvested. This might include hyaluronic acid, glycosaminoglycans (GAGs), and other protein, fat, and sugar molecules in the ECM. Our lab had unique access to decellularized tissue from the work of Dr. Alonzo Cook and his former PhD student Dr. Nima Momtahan. Weekly in the lab, porcine hearts harvested locally were decellularized by a process outlined and optimized here at Brigham Young University [43]. About half of the decellularized tissue would be used in a heart study seeding cells onto thin slices of the tissue, the rest was normally discarded. This residual tissue was used as the source for our dECM bioink following protocols from several other labs. Stephen Badylak's lab at the University of Pittsburgh was a pioneer in the area of decellularized tissues and his research heavily influenced the development of the optimized decellularization process done here at BYU. His research has taken decellularized tissue in several forms and applies them directly in surgery and in the manufacturing of a hydrogel [24, 44, 45]. Karen Christman, a professor at the University of California, San Diego has done a lot of research into decellularized organs and turning them into a hydrogel. The protocol to dissolve decellularized tissue discussed throughout several articles from her lab was very helpful in getting us started on our own protocol as well as other research reported on from her lab [46–51]. Most helpful in our efforts to make a dECM bioink was the work by Dr. Dong-Wo Cho at Pohang Universtiy of Science and Technology in South Korea. His work was most directly linked to our own as his goal was to 3D bioprint with a dECM. His other work was closely associated involving cross-linking techniques and developing vascularized tissue [23, 52–54]. The Cho lab's protocol dissolves the

ECM in a way very similar to the Christman lab. However, the application of the printed bioink in the Cho lab involved an extra support ink which we did not want in our bioprinting process, so our final protocol did not match exactly with the Cho lab. Our final protocol to develop a dECM bioink is an agglomeration of the research done by these labs as well as a lot of trial and error done in the lab here at BYU.

The protocol starts with the decellularization of the tissue which we will cover briefly. The process of decellularization generally consists of breaking down the cell membranes while keeping the ECM intact. Detergents and enzymes are used in conjunction with hypertonic and hypotonic solutions that breakdown and then cyclically shrink and swell the cell. This combination breaks down the cells and washes them out while keeping the ECM intact. Various researchers have published different protocols on decellularizing tissues including muscle and bladder [43, 55, 56]. In our lab, porcine hearts are harvested locally, cleaned, and frozen until needed for the weekly decellularization. The hearts are thawed and then hooked up to a peristaltic pump and various solutions are pumped through the heart as described above. This process takes the cells out of the tissue and leaves the ECM, which is needed in the dECM bioink. After the tissue has gone through the decellularization process it needs to be dissolved and broken down. Specifically, the collagen needs to be broken down to an un-cross-linked state where it can be cross-linked again by a thermal treatment. To do this we started by following the protocols discussed above from the Christensen and Cho lab along with several other labs which did similar processes [57–59].

Protocol

1. Blend decellularized heart tissue

   This is done in a normal blender and allows the dissolution of the tissue to happen faster when the acid and pepsin are added. Could also be a method in larger scale productions where the tissue could be homogenized with other batches to eliminate variety among the source tissue.

2. Filter blended tissue through cheese cloth

   The blended tissue was filtered through a simple cheese cloth so that as much water as possible could be eliminated from the tissue. This is so that a consistent collagen concentration

could be made each time and the concentration could be made more specifically to what we wanted. After the dissolution that happens next it is very hard to concentrate the collagen further by eliminating water, but it is simple to add water and dilute it down, thus we tried to get the highest concentration possible initially.

3. Combine tissue with 0.5 M acetic acid and 50 mg pepsin/10 mL blended tissue.

   The dissolution of the ECM is done partially by the acid, but mostly by the pepsin enzyme. Pepsin is uniquely activated at low pH and thus works well in this environment. The 0.5 M acetic acid concentration is achieved by adding in stock acetic acid directly to the tissue mixture that has been drained. This does not initially create a 0.5 M solution becuase there is not enough water to dilute the acid to that concentration, however, after the enzyme does its work more water is released from the ECM and the final volume of water does bring the acetic acid concentration to 0.5 M. This was determined to be the most effective method to keep the collagen concentration high in the bioink and not dilute out the collagen. The optimized mixture added 0.278 mL of glacial acetic acid to 10 mL blended tissue, which after mixing provided the water necessary to achieve the 0.5 M acid concentration.

4. Mix for 48 hours

   The mixing was done in a 50 mL conical vial with an improvised mixing system similar to the set up of a continuously stirred tank reactor. This consisted of an externally mounted electric motor with a power supply attached to a mixing shaft that stirred the mixture continuously for the duration. This was chosen over a magnetic stir bar becuase the mixture was too viscous for the stir bar to reliably mix the entire volume.

5. Filter dissolved mixture through cheese cloth

   The mixture was filtered through a second clean cheese cloth to pull out any undissolved tissue or other foreign particles that may have been present in the original tissue. This needed to be done carefully however as there was insoluble collagen in the mixture that is easily separated out but is vital to the successful cross-linking of the final bioink.

6. Add pH indicator and 1mL 10x PBS

The pH indicator is very helpful in the next step where the pH is changed to a physiological pH of 7. The PBS is added to return the salt mixture back to physiological conditions after the original washing of the ECM that happened during the decellularization process. We later found out that this step may not be needed due to the breakdown of the ECM and subsequent release of ions which raises the osmolarity higher than initially expected. However, it is very difficult to ascertain the exact osmolarity of the dissolved collagen mixture to know how much PBS needs to be added and more research needs to be done in this area to find a consistent way to achieve an osmolarity of 300 mOs. The addition of the PBS or water here is the place where the solution could be diluted down for different collagen concentrations, however in most of our work we used the highest collagen concentration possible to maximize the strength of the post-cross-linked prints.

7. Add 10 M NaOH to change pH to physiological conditions

   To not dilute the bioink, a high concentration strong base was chosen to change the pH. This was very effective, but troublesome because very small volumes made dramatic changes in the pH, particularly when getting near the equivalence point. Additionally, the dECM bioink will not cross-link at low pH, but when it is raised to above a pH of 6 the collagen will cross-link at room temperature. This means that the pH change needs to be done in refrigerated conditions of below 4 °C to ensure the collagen will not cross-link when the pH is changed. Practically, this was accomplished with a tub of ice water that the dECM bioink could sit in while the pH was changed dropwise with the base.

8. Centrifuge bioink in refrigerated conditions at 3000 rpm for 5 min

   Given the pH change made it possible for the collagen to cross-link at temperature above 4 °C, all further processing had to be refrigerated. The centrifuge step pulls out bubbles that accumulated during the processing of the bioink, the initial mixing and the pH adjustment, which can make the bioink less predictably compressible and require more adjusting of the printing parameters when using in the bioprinters.

This protocol, as mentioned above pulls heavily from the contributions of the Christman and Cho labs with slight differences. First would be the method of decellularization of the tissue.

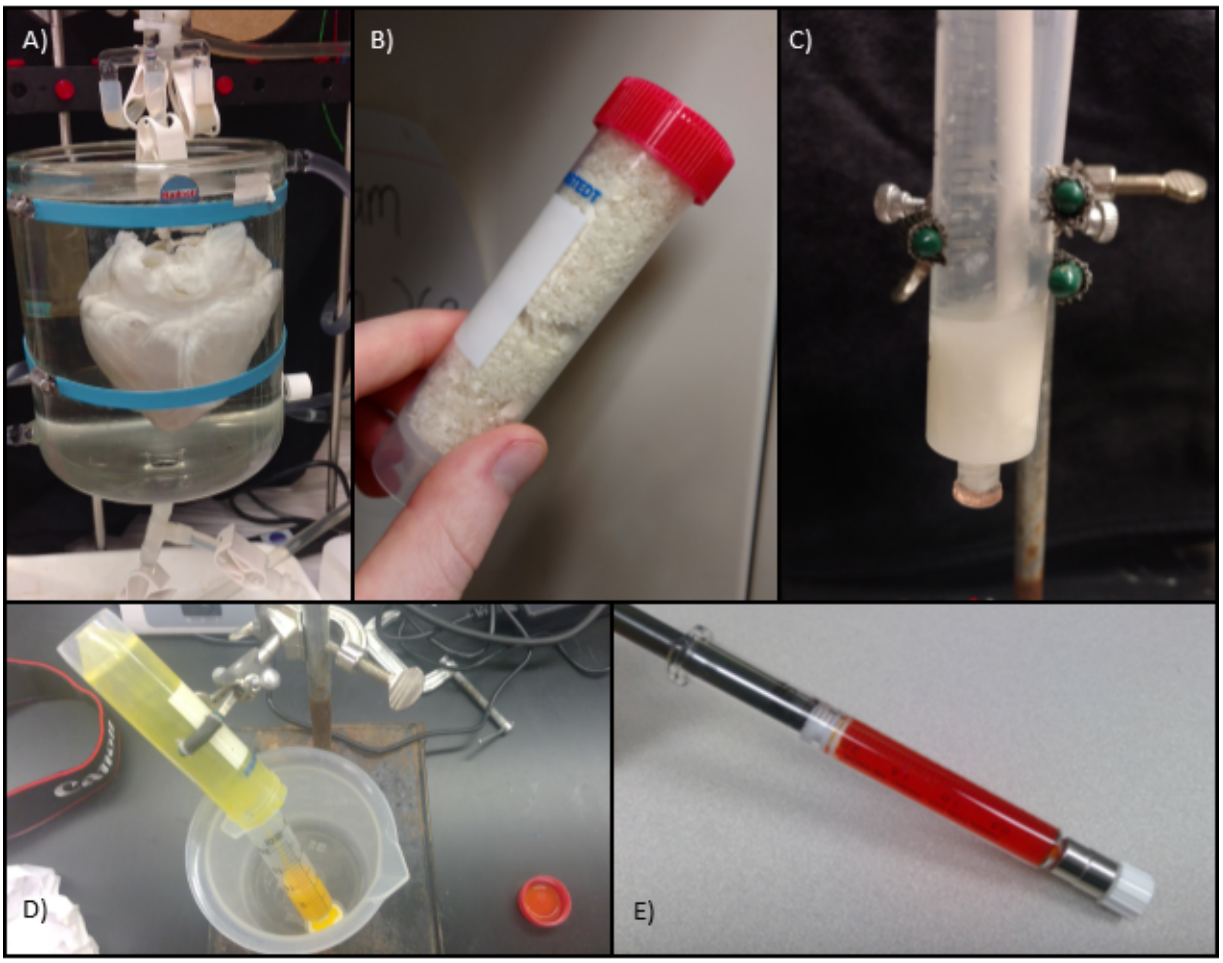

Figure 3.3: Process of making the dECM. A) Decellularized porcine heart B) Powderized and lyophilized decellularized tissue C) Mixing of bioink during digestion process by acid and enzymes D) Initial addition of pH indicator showing acidic bioink after mixing E) Finished bioink with pH changed to neutral.

The process our lab uses keeps the vasculature intact for later seeding of cells in other studies as shown in Ref [43]. This vascular structure is not required in our use of the tissue as the base for a bioink and is much more complex than would be necessary if the decellularized tissue were to only be used for a bioink. A simpler process is used by the Christman and Cho labs. Other differences include the use of the pH indicator and the purification process. Our use of a pH indicator, phenol red, made changing the pH much more practical, especially when the bioink needed to be kept cold to keep the collagen from cross-linking. The purification steps we took, including the straining and centrifugation, are unique and help to make the bioink process more repeatable and predicable.

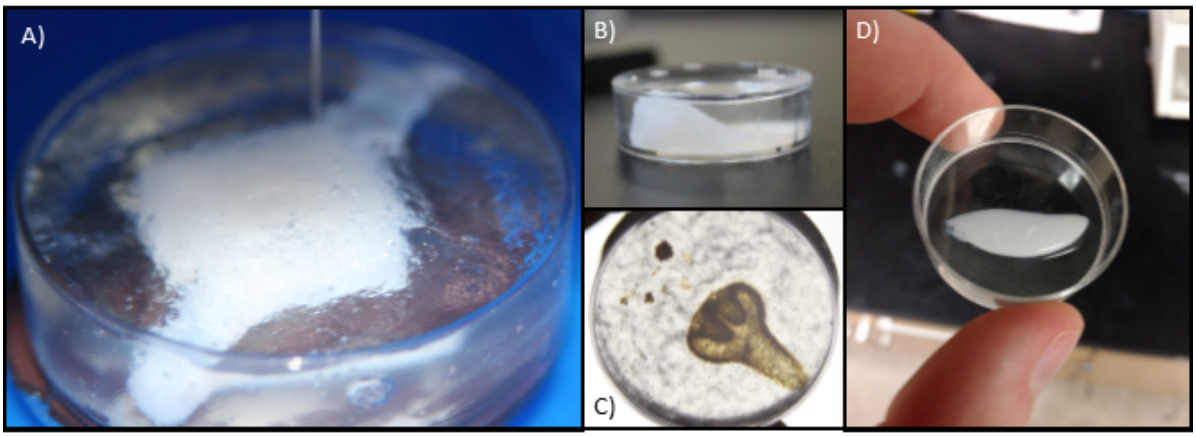

Figure 3.4: Bioprinted examples of dECM Bioink A) LifeCube with single inlet/out B-C) High resolution nose from side and below views D) Cross linked dECM bioink in air.

The next step in the formation of a working bioink was to sterilize the material and determine how cells act and grow in the bioink. We tried many methods of sterilizing the bioink, but no method worked well to preserve the structure of the uncross-linked collagen. Autoclaving the bioink denatures the collagen protein and does not allow it to cross-link later on. Radiation and chemical sterilization techniques that were tried proved to not be practical or not achieve the sterilization required. The method that ultimately worked was sterilizing the decellularized tissue initially before the tissue was dissolved and then keeping subsequent steps sterile.

3.5 3D Cell Culture Model and TissueBox Design

A true 3D cell culture, with cells placed in the right spots and a vascular system attached to provide support to the cells, is essentially no different from a native biologically derived tissue found in any animal or human. The real challenge comes in recreating that 3D cell culture environment, and successfully doing that may still be decades away. However, if we could recreate the 3D cellular environment, then a 3D cell culture made in the lab may be able to replace an animal model for drug testing. If it were good enough, it may even be able to stand in the place of human testing, if we can really recreate that environment. On the way to that goal of recreating the 3D cellular environment, one of the first benchmarks will be to create a vascularized 3D cell culture. The current holdup in 3D cell culture is essentially a plumbing problem. It is not possible to provide the flow of cell culture media necessary for cell survival to all of the cells in a bulk environment.

In native tissues, the standard for a diffusable distance where nutrients and waste can travel from a capillary to the farthest cell is about 200 μm. This distance will likely increase in an immature cell culture with essentially no developed ECM, but cells will likely need to be within at least 500 μm of a cell media supply to survive and mature. This is why a plumbing system, or vascular network, is needed for 3D cell culture to become a reality. The best 3D cell culture we have now is in the form of cell spheroids which are very limited in size because of the diffusion problems that are created and the lack of nutrient/waste exchange for the cells in the center of the sphere. What we need to make 3D cell culture a reality is a vascular network, for media to flow to cells throughout the bulk of the cell culture and allow them to proliferate and operate in 3D. A good review of the current state of vascular tissue engineering, and what steps still need to be taken, was done by Gui and Niklason [60].

A study from the Rensselaer Polytechnic Institute in 2014 showed that two parallel 3D printed channels within a hydrogel with various cells and growth factors were able to form a capillary network between the two channels [37]. This study showed that it is not necessary to print a capillary network, which can reach a diameter as small as 10 μm, but a capillary network can be grown within a hydrogel and attach to larger channels that can be 3D printed. Similar studies show that angiogenesis, the formation of new blood vessels, can be accomplished with various cell types and growth factors in different hydrogels including fibrin [61, 62]. Combining these ideas, we developed a bioprinted 3D cell culture design with open channels for the flow of cell media and parallel channels arranged such that angiogenesis could establish a capillary bed between the inlaid channels. The first version of this design was termed the LifeCube as seen in Figure 3.5 A,B. It featured a single inlet/outlet to be attached to a peristaltic pump and a series of branches in 3-dimensions that formed the parallel channels where the angiogenesis could occur. It was printed in collagen, but was not tested with cells because of the sterilization challenges discussed earlier. This version was submitted with the bioink company Advanced BioMatrix as the basis for an SBIR grant using their bionks and our biopriting and cell culture capabilities. The SBIR was ultimately not funded, but the design continued to be developed as we developed our own bioink and our bioprinting expertise matured.

A later version of this concept was named the TissueBox shown in Figure 3.5 C,D The TissueBox has yet to be thoroughly tested, but remains as the culmination of all of our work and

experience in bioinks and bioprinting. The TissueBox is the best guess we currently have as to what a 3D cell culture may look like when approached from a 3D bioprinting point of view. It is a unit cell featuring a single open channel that can be stacked horizontally and vertically to achieve any thickness or shape desired. This unit cell is created from a structurally supportive alginate cage with a dECM bionk as the primary bioink and cell carrier. This design utilizes the structural advantages of alginate gels, discussed earlier, which can have a variety of stiffnesses depending on the alginate concentration and the native cell-friendly nature of the dECM bioink with collagen. The TissueBox would be printed in a FRESH support slurry with two different bioinks, the strucural alginate hydrogel, and the cell-laden dECM bioink. After printing, the construct would be placed in an incubator where the bioinks would solidify and the FRESH liquify and the construct could be attached to a peristaltic pump for cell media perfusion by a single inlet/outlet design with branches or attachment to a specially designed microfluidic device. If a system like this could be reliably made in the lab with a bioprinted vascular network and an induced capillary bed via angiogenesis then this would be the first real method of achieving a true 3D cell culture. Once this was proven to allow for cell proliferation and maturation, a variety of cell types could be included in the cell-laden dECM bioink for testing in this environment. Pancreatic beta cells could be tested and see how they respond to glucose levels in the perfusion media, or cancer cells could be allowed to mature in 3D and then treated with various drugs. The development of a true 3D cell culture method would revolutionize the way that we currently use cell culture and will be the next step in the progression towards an artificial tissue.

3.6 Conceptual Design of a Better Bioink

There may not be such a thing as the perfect bioink. It may be best to customize the bioink for each application you are using, for instance, if the goal would be to make artificial heart tissue then it may be advantageous to use decellularized heart tissue as the basis for the bioink. Or perhaps it would work best to use a certain blend of collagen for muscle tissue regeneration. There are some overarching principles that are starting to be established that every bioink will need to be based around.

The first principle is that the bioink should be almost entirely biodegradeable by the cells themselves. The goal is to have the cells completely remodel the scaffold that was printed and

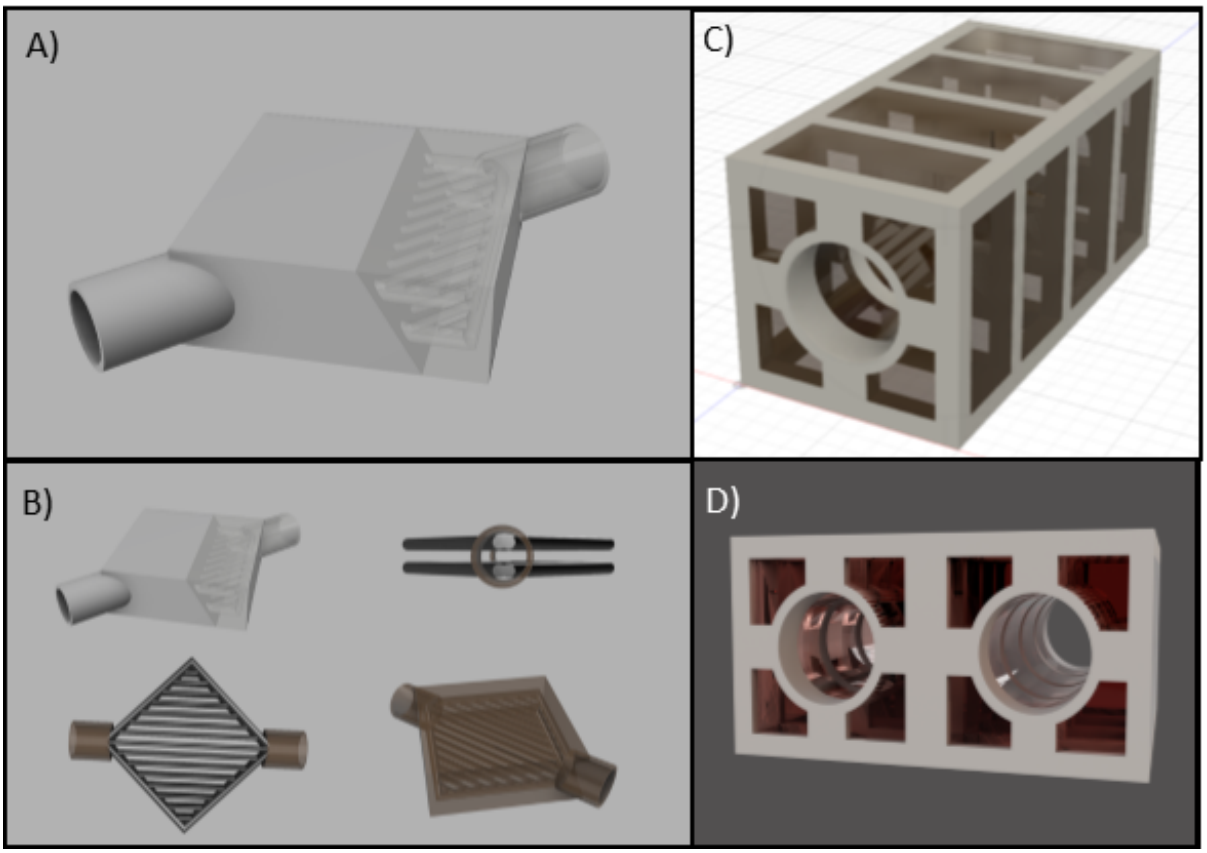

Figure 3.5: LifeCube and Tissue Box designs. A-B) Lifecube designs featuring a single inlet/outlet and a branched parallel channel network C-D) TissueBox design, individual unit with scaffold structure and multiple units in parallel.

replace nearly all of the material there with proteins and other ECM components. This means that the bioink either needs to be recognized and incorporated by the cells into their ECM, or used as a nutrient source that will be used up as the cells grow and proliferate. We tried to address this principle by mixing alginate and our dECM collagen bioink together. The alginate is partially biodegradeable in its ionically cross-linked form, but the MW of the original strands and the lack of the enzyme alginase in mammals creates problems in the total elimination of alginate [29]. Alginate is not a total solution by any means to the first principle, but may play a part in a totally biodegradable bioink.

The second principle is more obvious, that the construct to be implanted needs to be durable enough to withstand the stresses of surgery and suturing as well as the harsh environment it is implanted into. It is currently unclear as to when that implantation process should occur, or where the artificial tissue should be allowed to mature, in vivo or in vitro, but wherever that happens to

be, the printed construct needs to be durable enough at all points on the path to endure the process. This means that more than likely a structural element will need to be included in the bioink or printed as a second bioink to help maintain the structure of the print as it matures and the cells remodel the structure. As with the first principle, alginate may work well for this purpose because of the strong structural role it can play when it is used in high enough concentrations. However, the cross-linked alginate, even at the highest concentrations, is not an objectively very strong material, only in regards to other hydrogels. In conjunction with the first principle, this structural material will need to be biodegradeable as well as provide structural support. There are several polymers that may work well for this, but those would also need to be bioprinted and cross-linked to work in this kind of process. Fibrin may be a possible material choice which has already been 3D printed many times and used as a biodegradeable hydrogel in cell culture [**?**, 63, 64].

The third principle is similar to the second, that the cross-linked bioink needs to be soft and porous enough to allow the cells to be unconstrained in their proliferation. In current 2D cell culture, there is no scaffold for the cells to fill, there is only a roughened up surface for the cells to attach to as they proliferate, but they are proliferating in essentially a water bath with no obvious physical hindrances to their growth. When you add a 3D scaffold to the mix, things get more complex because you are adding a third dimension for the cells to proliferate into and attachment surfaces beyond the 2D plane, but at the same time you add obstacles in the way of the cells that may deny free-floating cells the path to attach to surfaces in that third dimension. However, this does not seem to be an issue for commercially available skin scaffolds sold by Acell (acell.com) which cover various dermal wounds and provides a and cell-free scaffold that decreases healing time and scar formation. More research needs to be done likely with cells once the demands of principles one and two are met to see how the cells will migrate through the chosen material.

These three necessary principles highlight why a good bioink is so hard to develop. The ideal cell-carrying bioink will need to be porous enough to allow for cell proliferation, strong enough to be sutured to, and biodegradable such that the cells can remodel the scaffold structure. All of these principles have not yet been optimized in any combination of bioinks that we are aware of, but these principles can help to guide us towards certain material choices.

CHAPTER 4. BIOPRINTER PARAMETER OPTIMIZATION AND RESOLUTION ANALYSIS

4.1 Background

4.1.1 Feedback Methods

One of the most difficult parts of additive/subtractive manufacturing is resolution and tolerance analysis to determine how the finished product matches the designed model. When machining aluminum for instance using a computer numerical control (CNC) machine, the finished part needs to be measured and compared to the original design to ensure it falls within specified tolerances for that part. For a metal part that may be a time consuming process, but not difficult. The part is physically measured either electronically or manually and evaluated or the part is compared to a specially designed and machined tolerance part which fits on/in the newly machined part and is able to quickly identify if the part is within specification. This method can be used to evaluate most traditionally 3D printed parts as well because they are generally hard plastic and can withstand that kind of evaluation. Additionally, in a 3D printing system you have instant visual feedback on how the process is going and can change parameters on-the-fly to improve the quality of the print or the print can be evaluated post-print and parameters changed to ensure that the optimal resolution is obtained. However, in bioprinting, this method of resolution analysis and parameter optimization cannot be done for several reasons. First, the final printed constructs aren't durable enough to handle and measure in a traditional sense. It isn't possible to take a collagen print out of the liquid bath it is in and measure it with calipers to determine how it matches up with the designed model. Additionally, the prints aren't stiff enough to hold their own weight in air, but tend to flatten out in air and resume their original shape in an aqueous media. Therefore any physical means of simply measuring the prints is not an option. Second, the printing process, as discussed in Chapter 3, is generally done in a printing substrate such as a carbomer or the FRESH gelatin slurry. This limits

visual feedback and doesn't allow for on-the-fly changes to printing parameters. In conjunction with this, the cross-linking process can slightly swell or shrink the print and give false feedback if the operator doesn't fully understand what is happening as the cross-linking happens. These two problems make identifying sources of error and correcting them very difficult. To use an analogy, bioprinting is like trying to make and bake bread using mechanical arms from the other room, and the only visual feedback you have is through frosted glass. If you get a salty lumpy loaf you aren't sure if the problem is in the making or the baking or some combination of the two, you only know the instructions you put in, and the final product that comes out. This is the challenge of parameter optimization and resolution analysis in bioprinting.

4.1.2 Current Methods

The unique problems encountered in bioprinting discussed above have not yet been fully solved, but techniques have been developed to address some of these issues. Investigation has been done in detail on the viscoelastic properites of shear-thinning hydrogels, which includes collagen, which helps to predict how these hydrogels will act when extruded and can be helpful in modeling bioprinting [65]. Characterization of a ceramic paste used in bone tissue scaffolds has been characterized in detail by researchers, but this was using microscopic visual confirmation which is not as useful when printing less solid pastes in a support substrate [66]. Other researchers have developed a method to optimize parameters of hydrogels in a very quantitative way which shows promise [15]. One proposed method is to use non-contact measurement devices like an MRI, but a traditional 3-tesla MRI machine only has about a 1 mm resolution, which is not a fine enough resolution when trying to print open channels in the 100 μm range.

A method to characterize 3D printed soft material constructs has yet to be developed. Such would allow for printing parameters to be optimized by providing feedback on prints and iterating print upon print. We set out to find a way to obtain feedback from the printing process to close the loop on the printing feedback system and optimize and quantify the resolution capabilities of any bioprinter.

4.2 Gelatin Embedded Resolution Analysis

Initially, what was most needed was a method to measure the printed constructs and quantify the resolution in some way. The first method we tried was based on the histological evaluation of tissue slices. In histology, tissue samples are processed such that they can be thinly sliced and then evaluated at the cellular level. We hypothesized that the same method could be utilized to evaluate the printed constructs and measure open channels that were printed and quantitatively define the resolution. The way that traditional histology is accomplished is with a series of dehydration steps where the existing medium in the tissue, starting with water, is slowly mixed with another fluid, such as ethanol, that it is miscible with and replaces the first medium. This process is then repeated with other materials until the tissue is finally imbued with a warm wax, which can be cooled or frozen and sliced thinly. With help from the lab of Dr. Paul Reynolds, we attempted to run our printed constructs through the same process as regular tissue. This method did not work as the prints were too fragile to survive the entire process. The first time this was attempted only small pieces of the original print survived, which was not sufficient to get a good evaluation of the resolution. After some discussions and research we tried again using a more gentle dehydration process used for the histological analysis of embryos which are fragile by nature. This process had similar results and the printed constructs did not survive the process. This is because the prints are very weakly cross-linked thermally and the collagen is not at all as strong as it is in native tissue in this state. We tried simplifying the process even more and taking advantage of the porous nature of the printed constructs, which were not nearly as dense as native tissue used in histology, so we hypothesized that the dehydration could be done in a single step. Finally we ended up using a VWR Premium Frozen Section Compound which is miscible with water and freezes to a consistency similar to wax that can be sliced via a cryostat. After printing and cross-linking, the constructs were placed in a 50/50 mixture of water and the freezing medium for 4-6 hours and then placed in a pure freezing medium bath for 24 hours in the refrigerator. This allowed sufficient time for the water to be replaced by the freezing medium and for clean slices to be taken with the cryostat. Cryostat sectioning then was done with slices tested from 50 - 200 μm. This method was mildly successful, and with further refinement could be a method to consistently get resolution feedback from bioprinted constructs, but there are several issues. First, it is very difficult if not impossible to prevent distortions in the final slices due to the embedding process and the fragility

of the slices after printing. What often occurred was that a good slice would be taken from the embedded construct, but in the process of moving that slice to a glass slide, the sample would become distorted in some way as the freezing medium melted.The print was not strong enough to hold itself together and return to its original shape when it was sliced so thinly. Also, when a good slice with minimal distortion was obtained, it was difficult to define the edges of the bioink. The edges tended to be very ”fuzzy” and measurements could vary with 1-2 mm differences depending on where a researcher chose to take the measurement. Lastly, the process was long and tedious, and it took at least 24 hours to obtain results from a print and try another iteration on the printing parameters. We concluded that although this method may work if it were refined and modified further for this application, it was not useful and practical to obtain resolution measurements for bioprinted constructs.

4.3 Raspberry Pi Camera Feedback System

While the gelatin embedded resolution analysis procedure was being investigated, we tried several other methods of evaluating bioprints. One was a simple procedure to look at printed and cross-linked prints under an optical microscope. A design shown in Figure 4.1.A called the BioBenchy, because of its use as a benchmark for bioprinting parameter optimization, was used which featured various shapes cut out in cookie-cutter fashion which created vertical channels of different shapes and sizes. These were then visible through a microscope and could in theory be measured and compared to the original design. Samples of pictures taken using this method are seen in Figure 4.1.B.

The method seemed to work, but the particular objective in the available lab microscope did not provide a wide enough field of view to obtain the images needed. Also, a consistent field of view from a camera that provides a digital image would have been desirable over the manual microscope that we had access to at the time. Modifications to the lab microscope were evaluated, but a different approach proved to be more valuable and cost effective. Dr. Gregory Nordin, when consulting on the cytotoxicity project discussed in Chapter 5, mentioned his lab making a microscope from a Raspberry Pi camera and he was kind enough to give us some direction on making our own. Using a Raspberry Pi and a plug-and-play camera attachment we were able to design a camera system with which to evaluate bioprints. The camera system is seen in Figure

4.1.C and is mounted to the bed of the bioprinter looking up. The camera sits horizontally and the plane of the field of view sits at the bottom of the petri dish holding the substrate for printing. The camera attachment for the Raspberry Pi features a focus lens, and with some trial and error using a 3D printed case/stand the focus plane was set to the bottom of the petri dish so that when a print is started, the first layer that is laid down is in focus. This turned out to be a good method to evaluate bioprints, but was actually more useful than initially anticipated because it also allowed for a live view of the first crucial layers of the bioprinting process. Figure 4.1.D shows what kind of images could be obtained with this setup, and the videos were also of immense help. Seeing that this method worked so well, we later invested in a small USB microscope which was also used to do the resolution analysis. This allowed us to get exactly the images that we needed with higher resolution than the Raspberry Pi camera could reasonably achieve. Example pictures with the associated measurement analysis are shown in Figure 4.1.E-F. With this new feedback method we were ready to establish a protocol that could ensure a bioprinter is repeatedly performing at its optimal resolution, and what that resolution is.

4.4 Optimization Procedure

4.4.1 Slic3r Settings and Variables

The process of setting up a bioprint is fairly straightforward until the slicing stage. Initially a CAD design is exported as an STL file, which is essentially an approximation of the CAD design built from triangles. This STL file can then be imported into a slicing program. There a lot of slicing programs out there, but one of the oldest and most advanced is called Slic3r which can be downloaded at https://slic3r.org/. This slicing program takes the STL design and cuts it into 2D slices that are stacked up to make the desired figure. The tool path is then calculated for each 2D slice in the stack. There are quite a few parameters to consider in this process like how thin the slices should be, how thick of an extrusion path do you use, how closely do you put two extruded paths next to each other so that they bond without too much overlap? The optimization of these parameters defines the resolution of the bioprinter. What makes this optimization particularly difficult is that there is no available software that specifically deals with bioprinting on an in-house device like ours. Commercially available bioprinters have their own software, but even that is not

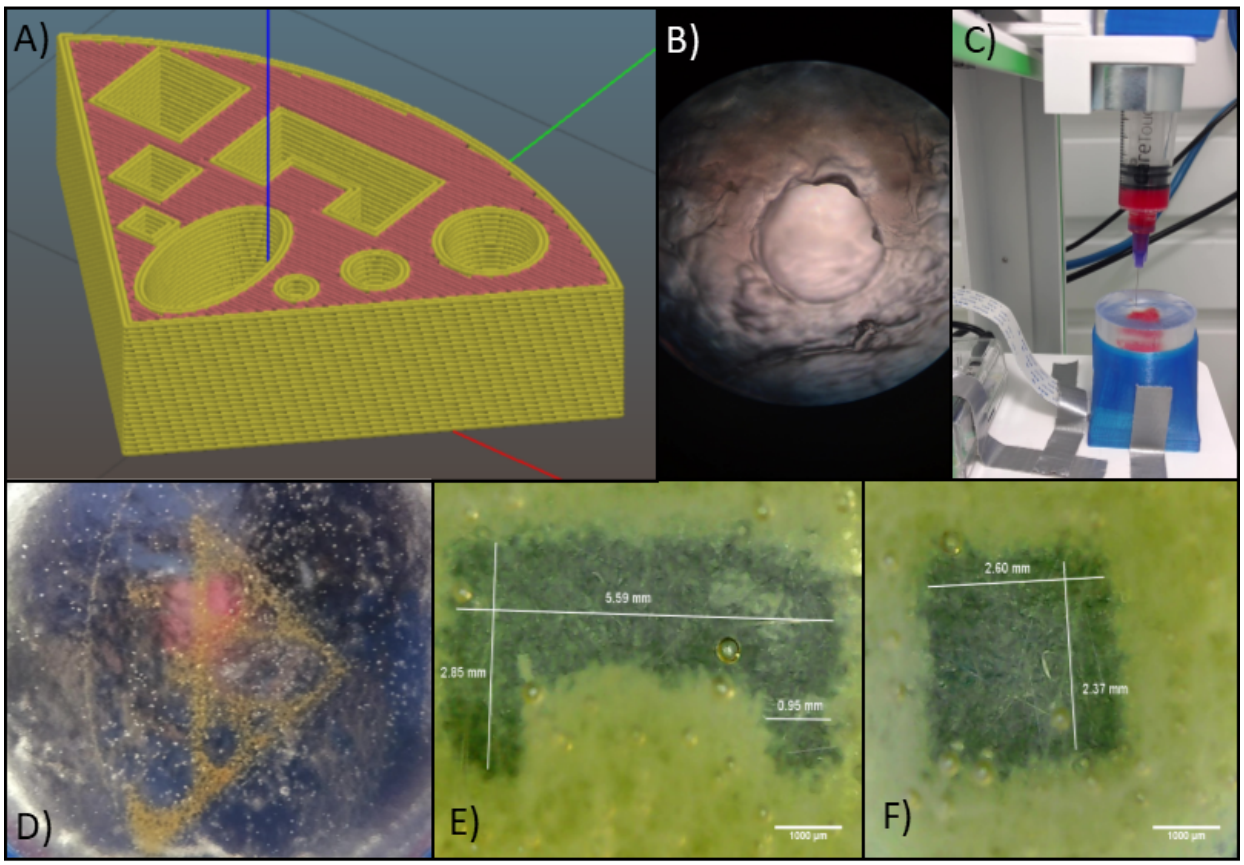

Figure 4.1: Camera Feedback System. A) Biobenchy design used as a benchmark for bioprinting resolution B) Lab microscope sample image of a bioprinted channel C) Raspberry Pi camera system attached to printing platform, duct tape was used to attach it to the bed D) Example of live images obtained from the camera system E-F) Biobenchy analysis using USB microscope and measurements taken.

transferable to printers that run on different motherboards or have different extruder setups. The Slic3r program we used is built for traditional 3D printers, and thus needs to be dealt with in a unique way to work for bioprinting.

There are essentially eight parameters in the Slic3r software that need to be set, and four of those need to be optimized for the particular bioink and printing substrate used. These parameters essentially define the model of the cross section of the paste extrusion coming out of the needle tip. Correctly optimized model parameters in the slicing software would match the slicer model with what is really happening at the printer, and have the goal of lining up those extrusion just right so that they bond to each other in a horizontal 2D layer and vertically layer upon layer. The parameters are laid out in Table 4.1 with a brief explanation of what they do in the software and relate to in

Table 4.1: Parameter Optimization Variables used in Slic3r

Variable	Explanation	Status
Extrusion Multiplier	A scaling factor for the extruded volume after the cross sectional volume is calculated. Used to correct the width of the extrusion when the calculated model is not accurate to reality	Optimized
Retraction Settings	The amount the syringe plunger is pulled back and then forward again to reduce the "stringing" effect that can happen during non-extruding moves	Optimized
Slice Height	The height of slices used by the slicing program to approximate the model in 2D slices	Optimized
Infill/Perimeter Overlap	A percentage overlap between the infill and perimeters calculated in the slicing software	Optimized
Nozzle Diameter	Inner diameter of the needle	Fixed
Extrusion Width	Width of the extrusion used to calculate the volume of an extrusion	Fixed
Filament Diameter	Diameter of the plunger or inner barrel of the syringe	Fixed

the printing process itself. Figure 4.2 is also supplied for a more visual representation of what the parameters relate to. The parameters that need to be optimized are the Extrusion Multiplier, Slice Height, Infill/Perimeter Overlap, and Retraction. The following procedure provides an opportunity to systematically optimize and quantify each of these parameters.

4.4.2 Water Test - Extrusion Multiplier Baseline

The purpose of this test is a baseline Extrusion Multiplier that can be used in later tests. A perfect printer and extruder system will have zero losses from the motor to the extruded bioink, however that is almost never the case. Because mechanical losses exist in the gearing system from the motor, flexing in the plastic of the syringe, slight compression in the bioink, and steps/mm configurations errors in the motor firmware, the volume that is meant to be extruded from the syringe is not always true to what is intended. This test pushes a defined 0.5 mL of water out of the syringe and tests to see how accurate the stock printer is in pushing that volume out. Then the extrusion multiplier is changed over a range of values and the weight of the dish is recorded to establish a relationship between the extrusion multiplier and the recorded weight. The correct

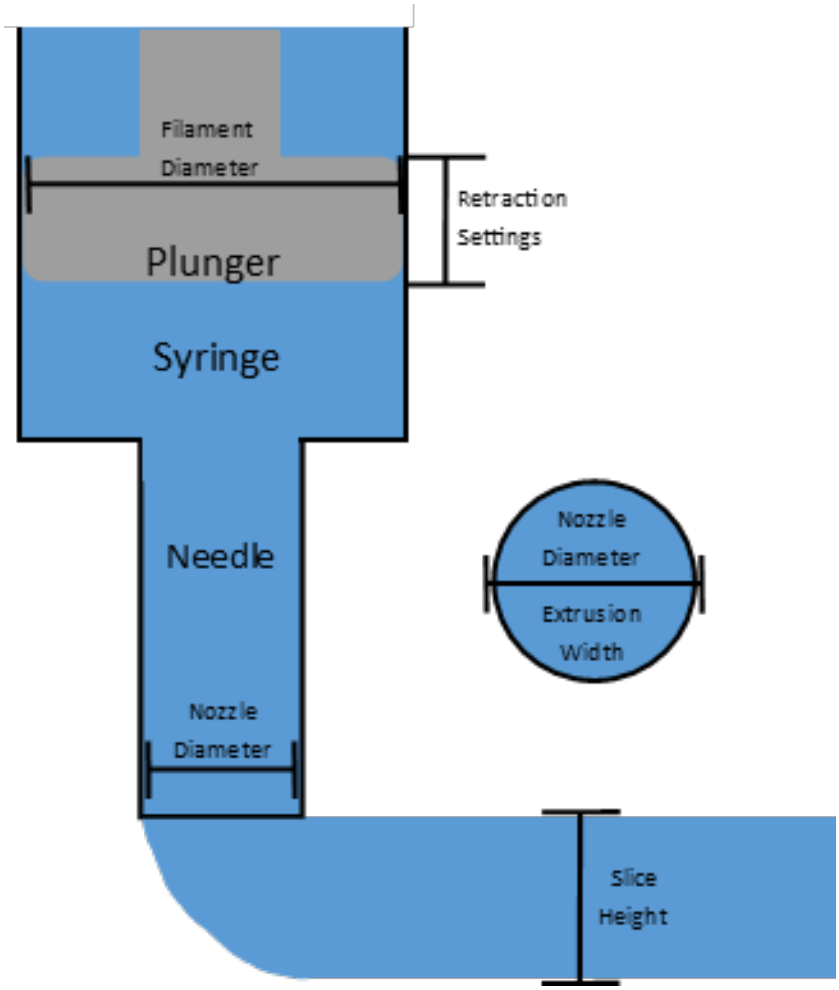

Figure 4.2: Physical representation of variables used in Slic3r program

baseline extrusion multiplier can then be recorded and the printer will have a correct designed to extruded volume ratio that accounts for losses in the system.

Procedure

1. Load test file and configuration settings

   The STL file provided named ”0.5mLBox.stl” can be loaded into Slic3r as well as the .config file provided to easily get the base settings needed for this test.

2. Update settings to reflect real needle and syringe

   Several settings will need to be updated to reflect the needle and syringe sizes that are used in the bioprinter being optimized. These setting can be seen by clicking on the ”Settings” menu

and selecting each of the submenus to view them, ”Print Settings”, ”Filament Settings”, and ”Printer Settings”. The following pictures show what settings need to be changed. The Red boxed values need to be changed to the inner diameter of the selected needle in mm, and the Blue boxed values need to be changed to the diameter of the barrel/plunger of the selected syringe. During these changes insure that the Extrusion Multiplier setting is set at 1.

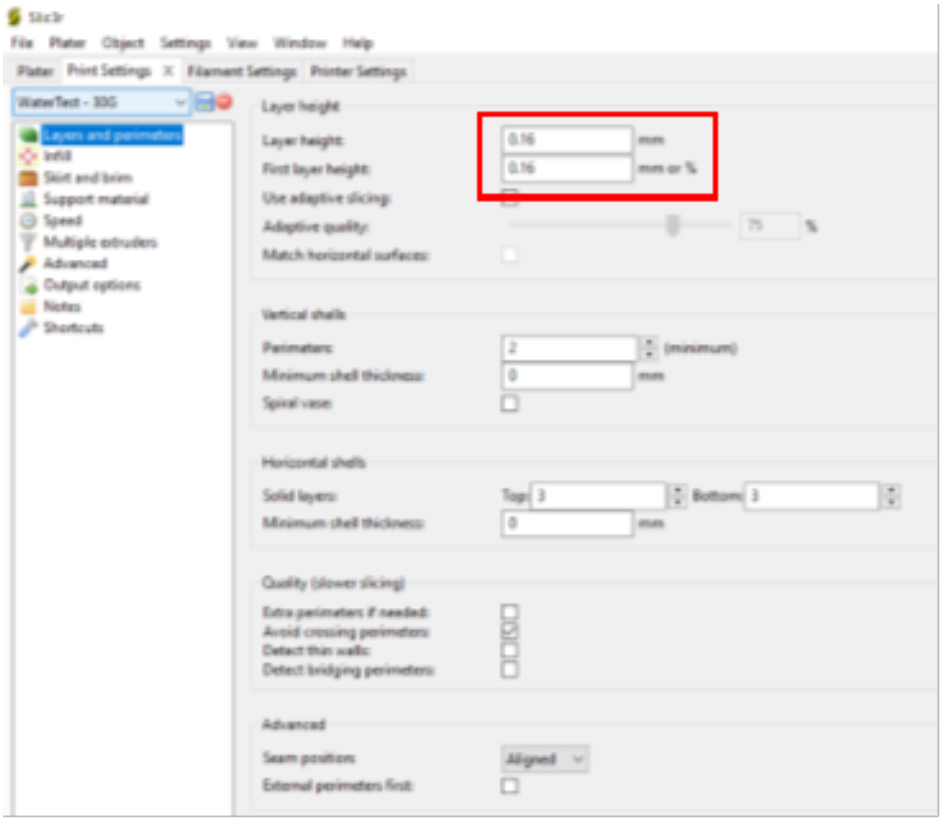

Figure 4.3: Slic3r Water Test 1

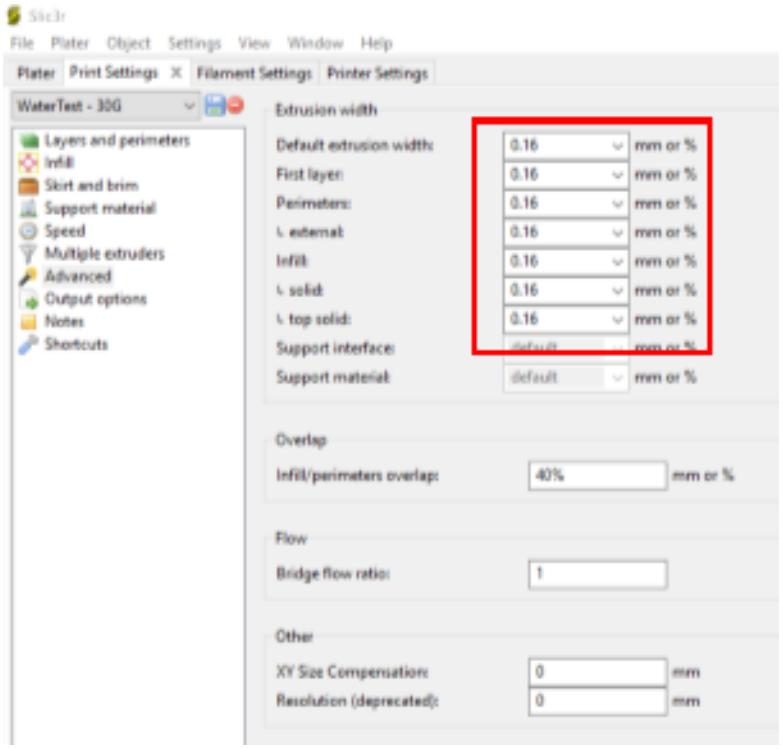

Figure 4.4: Slic3r Water Test 2

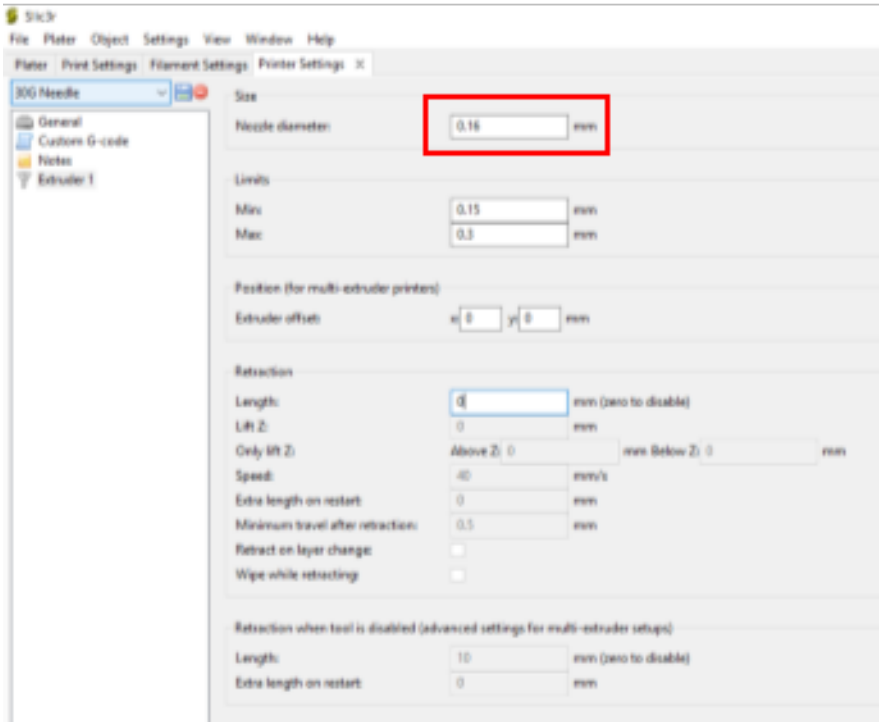

Figure 4.5: Slic3r Water Test 3

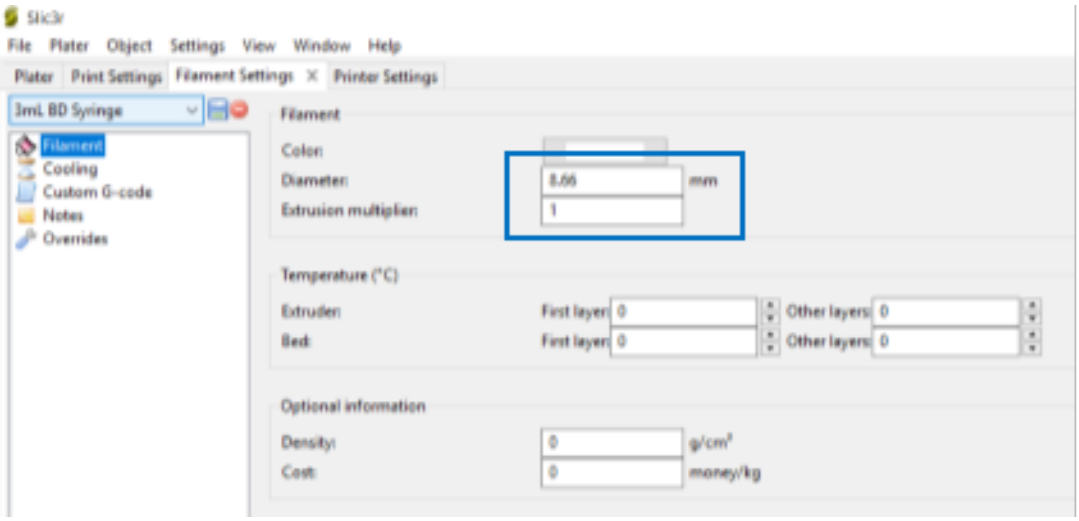

Figure 4.6: Slic3r Water Test 4

3. Choose speed and slice file

   After the settings are updated to reflect the real needle and syringe values, a speed can be chosen to print. This will make no difference in the test results and a speed faster than would normally be used to print, 10-20 mm/s is recommended to save time in the printing process. Slice the file.

4. Setup printer and petri dish, print file

   Get printer set up as normal and print using a 35 mm petri dish. A larger dish may be used, but this print is designed to fit inside this size dish. Fill the printing syringe with water and mount in the printer. Attach the needle and prime the needle such that water is just at the tip of the needle. If there is air in the needle and it is not primed the test will give false results. Weigh the petri dish and record the weight. Fit the dish in position on the printer. Load and print the sliced file.

5. Weigh dish with print

   After the print finishes, quickly weigh the dish and record the weight. Convert the weight to a volume assuming the density of water.

6. Repeat steps 2-7 until a wide range of data is obtained

At this point two methods can be followed. The quickest approach is to simply find the Extrusion Multiplier where the extruded volume matches the designed volume of 0.5 mL. This will require guessing a new Extrusion Multiplier repeating the test to see if the new value is closer in terms of the extruded volume. Repeat tests until the extruded volume matches the designed. A more detailed method can be performed where the extrusion multiplier can be varied over a range of values, 0.2 - 1.3, and plotting the recorded extruded volumes with their associated extrusion multipliers. This will provide a plot where the baseline extrusion multiplier can clearly be determined as shown in Figure 4.7.

Once determined, this baseline extrusion multiplier can give users an idea of how much loss there is in their printer/extruder system and where the Extrusion Multiplier provides a 1:1 ratio of the designed/extruded volume. Once optimized the baseline Extrusion Multiplier value can be input into Slic3r in the Filament Settings > Filament > Filament section. This parameter is only printer and equipment dependent, and therefore is valid for any bioink/substrate used. However, different syringes may need to be done separately because of possibly different losses within the syringe and plunger.

4.4.3 Retraction - Clean Starts and Stops

The retraction parameter moves the plunger of the syringe back slightly when non-extruding movements are made to prevent a common problem in 3D printing known as ”stringing”. This happens when the tool tip is moved from a location where it had been extruding to a new location, and on the way no extrusion is desired. If no retraction is done, then a spiderweb like strings tends to string from the nozzle tip and creates small undesirable imperfections in the print. In this step, the retraction setting is optimized by printing four parallel lines and changing the setting until the starts and stops of the lines are clean with no stringing. To successfully perform this step the user will need to have some familiarity with gcode. Gcode is the language that 3D printers and CNC machines run on and is quite simple to learn. Good online tutorials are available.

Procedure

1. Load provided gcode file in editor

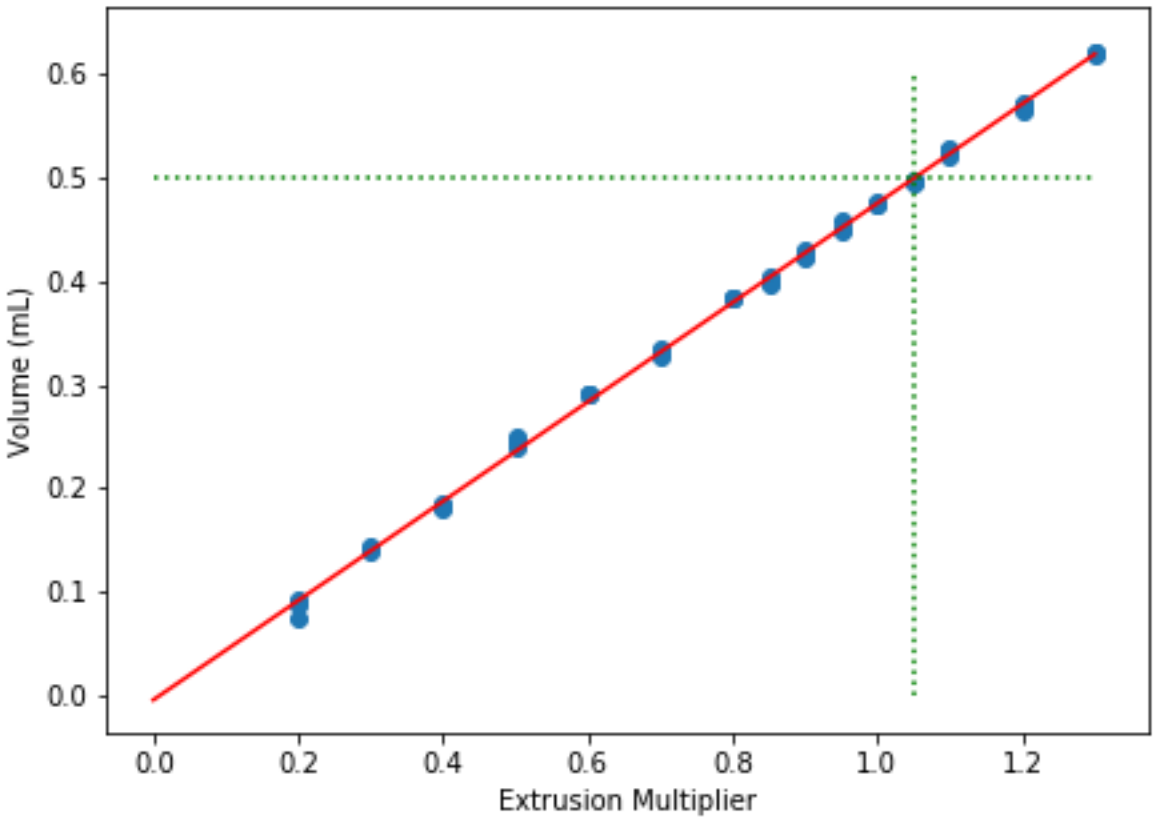

Figure 4.7: Baseline Extrusion Multiplier water test graph. The Extrusion Multiplier was varied through known values and the resultant volumes of extruded water were recorded. The graph provides a relationship between the Extrusion Multiplier and the extruded volume which should be linear. The baseline Extrusion Multiplier was then found by matching the Extrusion Multiplier where the 0.5 mL extruded volume was found.

Load the provided gcode file titled ”retraction.gcode” into a text editing software. Notepad++ is recommended and can be downloaded for free, but other text editors will work as well. At the top of the code in lines 4-6 there are three variables named Extrusion Amount, Retraction, and Prime. These variables are just placeholders for the values currently in the code and will need to copied to the rest of the code using the Find and Replace function when they are later changed. The Extrusion Amount is a default value based on an Extrusion Multiplier, found in the previous step, of 1.05. This value may need to be changed depending on the previously found baseline Extrusion Multiplier. In the end it simply needs to be extruding

enough to print a good solid line, the fine details of the Extrusion Multiplier won't affect this test. The other two variables, Retraction and Prime, are the current values that are found within the rest of the code for the distance the plunger is retracted before a non-extruding move (Retraction) and the distance the plunger is moved forward again when an extrusion is about to start (Prime). The values here will work initially but are the values that need to be optimized in this step.

2. Print initial test

   Set up a 35 mm petri dish on the print platform and center it such that the needle is at the center of the dish and zeroed at the bottom of the dish. The distance between the bottom of the needle and the petri dish is important to get right and consistent. Slide a piece of paper underneath the needle and move the print bed until there is some resistance from the paper when it is moved underneath the needle tip. This creates the appropriate gap between the needle and the petri dish. The print can then be started by loading the gcode file. Other modifications may need to be made to the file depending on your print settings, but that will be dependent on the printer and will require a good knowledge of gcode to adapt.

3. Evaluate test and change parameters

   Figure 4.8 shows what an unoptimized vs optimized test looks like. Repeat steps 1-2 until the test has clean starts and stops with no stringing as shown in the figure. This can be done without the camera setup described above, but is made easier with it. Record the optimized retraction and priming values.

By optimizing these retraction settings, stringing will be eliminated or minimized which creates cleaner prints and predicable results. Copy the optimized values in to Slic3r in the Printer Settings > Extruder > Retraction section. The "Length" value correlates with the Retraction setting, and "Extra length on restart" is the Prime value. These settings are dependent on the syringe, needle, and the bioink used and will need to be optimized for each combination.

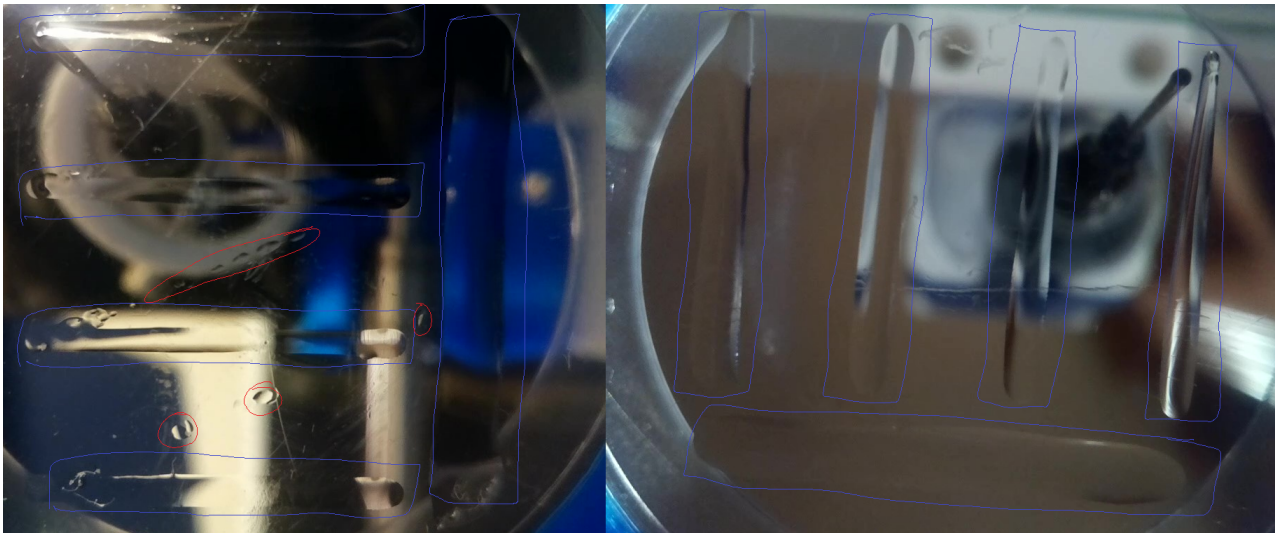

Figure 4.8: Retraction settings optimization results. Four paralell lines test for clean starts and stops. Left: Un-optimized settings, red shows residual stringing. Right: Optimized settings which show clean lines with no stringing.

4.4.4 Extrusion Multiplier - Solid 2D Layers

This step ensures that solid 2D layers are being formed by changing the Extrusion Multiplier from the baseline value. The reason that this value needs to be changed is because of the shape of the cross section that is being extruded from the needle tip. The assumption in the slicing software is that the cross section is circular with the same diameter as the inner diameter of the needle. This however is not often the case because of the attraction of the bioink to the needle. Metal needles are highly wettable and the bioink, which is aqueous, tends to climb up the needle slightly which shifts some of the extruded volume upwards and creates a thinner cross section than intended. The Extrusion Multiplier then has to be increased to compensate. However, some bioinks, like alginate, tend to require a much smaller Extrusion Multiplier than the baseline value when optimizing using this method. This is thought to be because of the swelling nature of the alginate when it cross-links, but more research should be done to investigate the phenomenon.

In this step a print speed should be chosen that will remain consistent for the combination of needle, syringe, bioink, and printing substrate chosen for this optimization. The print speed affects the cross sectional area because a faster print speed will not allow the bioink to climb the needle as much as a slower print speed and will result in a flatter cross sectional area. Figure 4.9 shows simple Reynolds number calculations that vary the fluid velocity through the needle with the

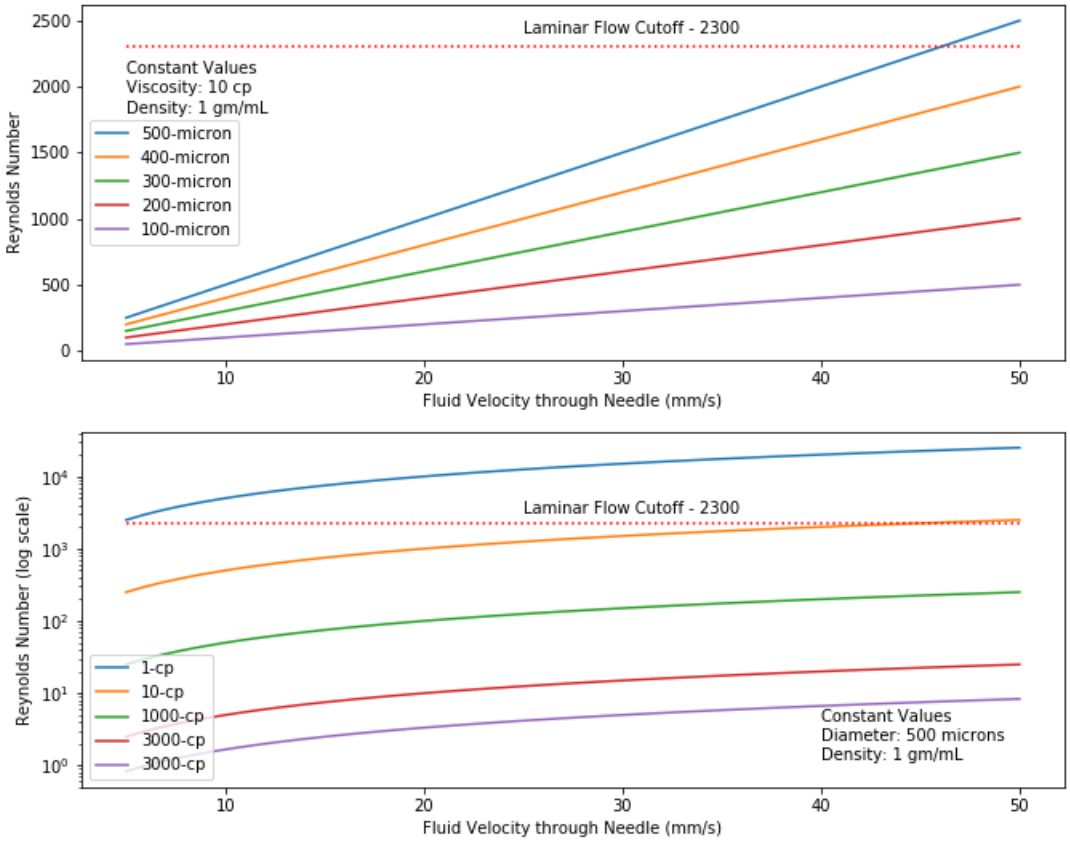

Figure 4.9: Reynolds Number calculations as a function of fluid velocity through various needle sizes and for various bioink viscosities. A print speed should be chosen that is within the laminar region so that the cross section of the extrusion is predicable.

corresponding Reynolds number for various needle diameters and bioink viscosities. This should help users get an idea of how their particular needle size and bioink affect the print speed they should be using. The fluid velocity should always be kept in the laminar region to ensure that the extruded cross section is predictable. The print speed is not shown on the graphs, but for a predicable cross section, should match the fluid velocities coming from the tip of the needle. We have found that 10 mm/s tends to be a safe speed for most bioinks. Whatever speed is chosen, be sure to record it and keep in mind that speed is attached to the optimized parameters determined in this step.

This step is best done with the camera system discussed above. This is because depending on the particular bioink and printing substrate combination used, the finished print may distort or the bioink may diffuse slightly before the print can be evaluated. The camera system allows live video/pictures to be taken and parameters can often be updated via intuition from watching the print even before it finished printing. However, the camera system is not necessarily required. The prints should also be allowed to finish printing and cross-linked to ensure that a solid layer is formed after the cross-linking process and the prints could be evaluated.

Procedure

1. Load the provided file and print

   Load the provided STL file named "SingleLayerBox.stl" and slice it according to the default settings that were optimized in the previous steps. It should be a single layer box that fits within a 35 mm petri dish. Whether the box slices as a single layer will depend on the set layer height. Change the layer height up so that a single layer is shown in the slicing viewport. The infill should be at 100%. Slice and export the file as gcode and print. Make sure the needle tip is centered at the bottom of the 35 mm petri dish. Choose a speed as discussed above and make sure that all values in the Slic3r Print Settings > Speed > Speed for print moves and Modifiers sections have that speed recorded. Set up printer and petri dish with the printing substrate and print.

2. Evaluate print and update parameter

   After printing evaluate the printed layer. This can be done with the camera system as discussed, manually by observing the bottom of the petri dish after printing, or observing after cross-linking. Any of these methods are adequate, but the fastest method would be using the camera system. After the print is evaluated, determine if/how the Extrusion Multiplier should be changed to create a solid single layer. This should be the lowest value of the Extrusion Multiplier that forms a solid layer so that a clean surface finish can be obtained and the printer is not overextruding. An example of what should be observed in a solid layer is shown in Figure 4.10, this includes parallel lines that just touch/overlap or the boundary

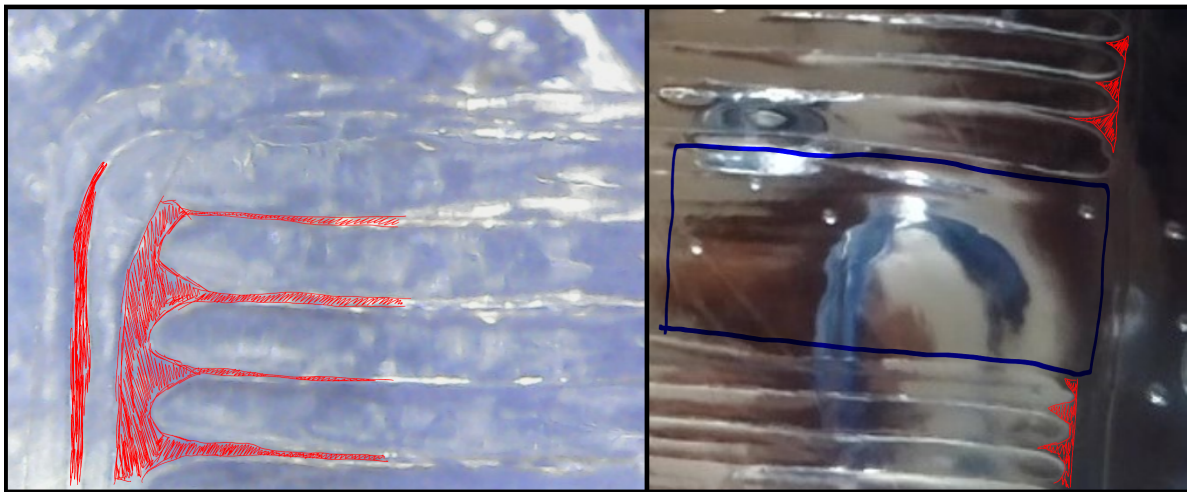

Figure 4.10: Extrusion Multiplier optimization results, Left: un-optimized single layer box print, the red shows void space that will not allow the 2D layer to bond well. Right: Optimized print, much less void space, blue region shows extrusion lines that have blended such that there is no longer a distinction between them.

between them disappears altogether. However, the most definitive test is done post-cross-linking so that the swelling of the print can be accounted for and all the extrusions can be seen to bond to each other.

3. Optional parameter - Infill/Perimeter Overlap

   During this test it may be observed that the infill bonds well together as well as the perimeter to itself, but there is a gap between the two. This can be solved by changing the Infill/perimeters overlap value found in Slic3r under Print Settings > Advanced > Overlap.

Record the optimized Extrusion Multiplier value and copy it into Slic3r in Filament Settings > Filament > Filament. This parameter is valid only for the particular needle size, syringe, bioink, and printing substrate tested.

4.4.5 Slice Height - Combining Layers

The last parameter to optimize the Slice Height which is a reflection of the height of the cross sectional area that is being extruded, accounting for some overlap so that layers bond well. This is the most difficult parameter to optimize because it is difficult to observe. There are several ways to test and optimize this parameter, but they all tend towards a subjective visual evaluation

vs a quantitative measure as can be done using the camera system in the other steps. This is a less desirable method of evaluation, but with some practice and a few steps the Slice Height value can correctly be obtained.

Procedure

1. Load provided STL file and print

   Load the provided STL file named ”SliceHeight.stl” into the slicing software. The model can be seen in Figure 4.11 and features a stair step pattern where individual layers can be seen and then tested to see if the layers bond to each other. Once loaded this file will need to be manipulated slightly to get the layers right from the slicing software. The end goal is to have each of the steps be a single sliced layer by scaling the print vertically (only in one dimension) and changing the Slice Height parameter in Slic3r under Print Settings $>$ Layers and perimeters $>$ Layer height. Make sure the ”layer height” and the ”first layer height” match each other. An inconvenient quirk of Slic3r is that for the correct cross section to be modeled, the Layer Height and the Nozzle Diameter parameters need to be kept the same. This means that when changing the Layer Height in this step, the Nozzle Diameter also needs to be changed to match. This defeats our original purpose of using the real needle diameter in the first step, but this is the only way to maintain the modeled cross section. The Nozzle Diameter parameters are under the Printer Settings $>$ Extruder $>$ Size section. Once this is done the file can be exported and printed as usual.

2. Evaluate print and update parameter

   After the print is finished, allow it to cross-link and evaluate it for layer upon layer adhesion. If the layer height is too small the surface will be bumpy and not clean, too large and the layers won’t bond to each other. When changing the Layer Height parameter, be sure to change the Nozzle Diameter as well to match. Repeat printing process until the optimal layer height is achieved. Record for use in Slic3r.

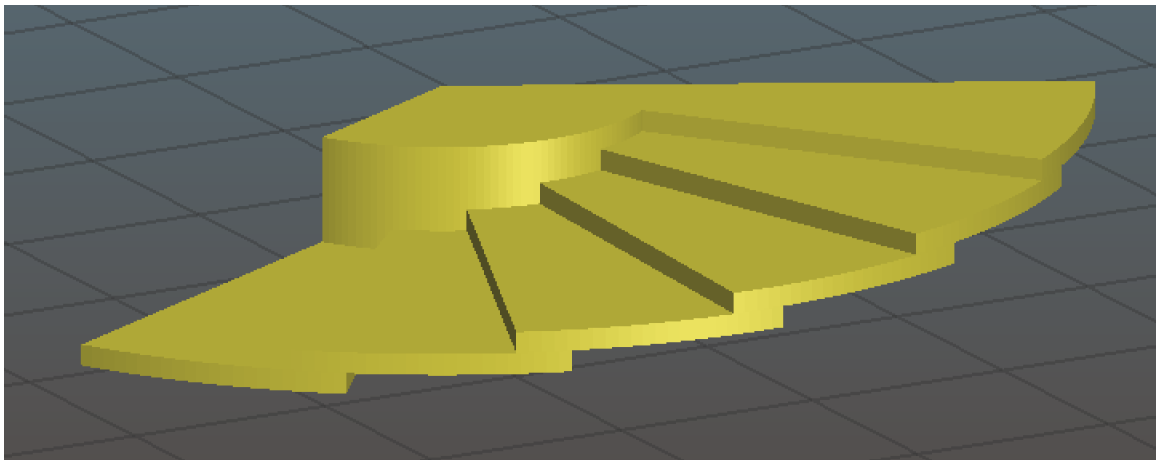

Figure 4.11: Slice Height optimization step model, features a single layer stair step design where single layer slices are printed with slight overlap to see the adhesion between layers and if a good layer Slight Height parameter has been reached.

3. Optional - Print tall box

   Another method to get the layer height is to print a tall box and observe the surface of the box and whether it has a concave or convex nature. This is an easy to observe phenomena, but takes longer to printer and more bioink is necessary to run the print itself.

After the Layer Height parameter is optimized the Layer Height and Nozzle Diameter can be changed in Slic3r. This parameter is valid only for the particular needle size, syringe, bioink, and printing substrate chosen in the test. It would also be logical to re-optimize the Extrusion Multiplier in the previous step since the Nozzle Diameter was changed here. In our experience this does not change the optimized Extrusion Multiplier much, but may have a slight effect.

4.4.6 Conclusion

With the previous step, a bioprinter can be optimized to achieve its highest possible resolution. That resolution is, however, hard to quantify exactly, and may be best expressed in the lumen diameter that can be printed. Most 3D printer motors have a resolution around 100 μm, however, the needle diameter will have the largest influence on the resolution of the printer overall as its diameter is typically around 100-500 μm. The reportable resolution of the printer will depend on these two parameters as well as the bioink and the printing substrate. A bioink that does not cross-link well will not be able to hold its shape well and reliably have clearly open lumens of a

particular size. It has been observed in our research however that <1 mm diameter lumens are achievable and within reach of an optimized desktop bioprinter.

CHAPTER 5. 3D PRINTED MICROFLUIDIC CELL CULTURE: CYTOTOXICITY AND CELL ADHERENCE ANALYSIS FOR PEGDA RESINS

5.1 Background

5.1.1 3D Printing Microfluidics

Microfluidic, Lab-on-a-Chip, devices are one method by which complex cell-based research can be simplified from a multi-step process to a single manageable step. Applications include stem cell analysis, cell-drug interactions, and as 3D cellular scaffolds as demonstrated by various researchers [67–72]. Biosensing devices have also recently been developed using microfluidic devices for preterm birth biomarkers [73]. However, manufactring of these devices is an expensive and slow process. Currently, commercially available off the shelf microfluidic devices compatible with cell culture cost anywhere from $150 to over $2000 (https://mimetas.com, https://alineinc.com). Polydimethyl siloxane (PDMS) is used in microfluidic devices with cell culture to make custom devices in the lab, but the fabrication process for these devices is slow (hours to days depending on complexity). Typically manufacturing custom PDMS devices uses cleanroom processes and molding (i.e., soft-lithography). PDMS has been extensively studied for cell culturing in microfluidic devices and its associated advantages and challenges have been elucidated [74]. Additionally, Lung-on-a-Chip [75] and Kidney-on-a-Chip [76] microfluidic devices have been made with PDMS and show promise in their respective applications with microfluidic cell culture, but the manufacturing of these devices in-house is a slow process.

3D printing allows for the rapid fabrication of complex geometries, and the Nordin lab at Brigham Young University has shown that 18 μm x 20 μm cross section channels can be obtained using a specialized DLP 3D printer and associated resin [13]. The poly(ethylene glycol) diacrylate (PEGDA, MW258) resin currently used in this printer includes a 1% (w/w) Irgacure 819 photoinitiator and a 2 % (w/w) 2-nitrophenyl phenyl sulfide (NPS) UV absorber. PEG itself is a

polymer well-suited for biological use given its native non-immunogenicity [77]. However, for use in biological applications, the photoinitiator and UV absorber require cytotoxicity analysis.

In this study, the photoinitiator Irgacure 819 and two different UV absorbers were tested in the PEGDA resin to evaluate their cytotoxic and cell-adherence properties. This study also evaluates post-processing methods to leech out cytotoxic species, thereby dramatically reducing the material's cytotoxicity.

5.2 DLP Microfluidic 3D Printer

The 3D printer used in this paper is described in References 13, 78, 79. It has a 385 nm LED light source and a pixel pitch of 7.6 μm in the projected image plane. We used a custom photopolymerizable PEGDA (PEGDA, MW258) resin as described above. Details about the development of this resin, and the motivation behind its formulation to produce the smallest stereolithographically 3D printed channels reported to date, are provided in Ref. 13.

We used 25 mm square silanized glass slides as 3D printing substrates. Slides were first rinsed with acetone and isopropyl alcohol (IPA), and then immersed in toluene mixed with 10% 3-(trimethoxysilyl)propyl methacrylate for 2 hours. After silanization, we stored the glass slides in fresh toluene inside a closed container until use, which ranged from under an hour to several weeks. All 3D prints reported in this paper were fabricated with a layer thickness of 10 μm. The image plane irradiance was 21.2 mW/cm^2 with an LED source spectrum as reported in [13] with a peak at 383 nm.

The design was a cylinder with a diameter of 13.1 mm and an average thickness of 146 μm as shown in Figure 5.1. It is worth noting that the printed chips were not perfectly circular, but cut along a chord on one side because of the 12 mm width of the available print bed. After printing, samples were flushed with IPA prior to optical curing, which consisted of a 30-minute exposure in a custom curing station using a 430 nm LED (Thorlabs, Newton, New Jersey) having a measured irradiance of 11.3 mW/cm^2 in the curing plane. After curing, the samples were soaked in DI water, which enabled them to be more easily separated from their glass substrates using a razor blade. The samples were then allowed to dry in air prior to use.

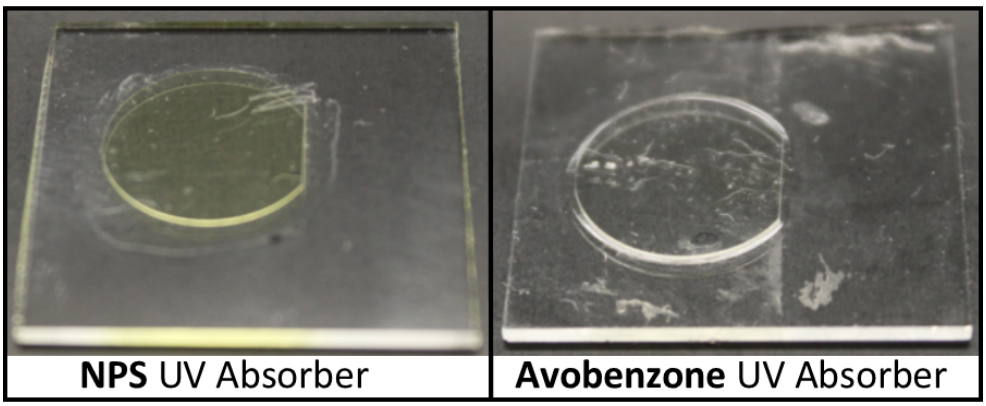

Figure 5.1: 3D printed PEGDA substrates for cellular cytotoxicity and adherence testing

5.3 Cytotoxicity Testing

The PEGDA material was tested using a direct contact technique as outlined in ISO 10993-5, which consisted of growing a cell layer on tissue-culture polystyrene (TCPS) and placing the material being tested on top of the cell layer. After 24 hours, the cells were stained with a Calcein AM/Ethidium homodimer live/dead assay (Biotium Inc.) and imaged to detect changes indicative of cytotoxicity. Stained cells were imaged using a FLoid Cell Imaging Station (Life Technologies) and images were analyzed and viability assessed using CellProfiler (CellProfiler.org). According to ISO 10993-5, a cell response was considered cytotoxic if there was a 30 % decrease in surface area coverage versus a control. Initial testing showed that the as-printed NPS PEGDA polymer, induced a severe cytotoxic response from the cell layer as seen in Figure 5.2.b. For initial cytotoxicity investigations, PEGDA substrates were printed with no UV absorber added, thus isolating the cytotoxic response from the photoinitiator Irgacure 819, and when tested with cells, no cytotoxic response was seen. It was thus concluded that the cytotoxic element of the resin was the UV absorber and cytotoxicity tests were performed with resin containing the UV absorbers.

PEGDA substrates were then printed using the Irgacure 819 photoinitiator and two different UV absorbers. NPS was used in prior publications [13, 78–80] and has been demonstrated to produce good prints with very high resolution, as mentioned above. Cytotoxicity tests were performed the the NPS containing resin with EA.hy926 cells (ATCC CRL-2922), an endothelial cell line, which were grown and passaged according to protocols established by the manufacturer. These cells were chosen over a primary or stem cell line because of their ease of use and low cost

of maintenance. This cell line is likely less sensitive to cytotoxicity than other cell lines, but the results show general cell behavior in the presence of strong cytotoxic contaminants. To leech out the cytotoxic constituents in the polymer,namely NPS the UV absorber, both water and ethanol were tested as possible eluents. DI water was chosen because of the nature of PEGDA and its common use as a hydrogel. It was also determined that 200 proof ethanol was a good eluent candidate given the higher solubility of NPS in ethanol and for its ease of use. Washing of the PEGDA substrates was done for up to 96 hours. Given the low solubility of the contaminants in water, the distilled water was changed out every 24 hours in order to not saturate the solution. Ethanol was not changed out during the washings.

The washed PEGDA substrates were then tested for cytotoxicity using the direct contact method and were stained using the Calcein AM/EthD live/dead assay and imaged for evaluation of fractional cell surface coverage. Results are given in Figure 5.2, which shows the fractional surface coverage of cells normalized to TCPS seeded at the same cell density. Eluent tests showed that the 3D printed PEGDA resin containing NPS as a UV absorber could be made non-cytotoxic by an eluent wash. A DI water wash showed that after 48 hours the level of NPS in the substrate was reduced such that the substrate did not induce a cytotoxic response as shown in Figure 5.2b. However, the ethanol wash proved to be more effective and achieved a non-cytotoxic response after only a 12-hour wash, as seen in Figure 5.2a. Washing with ethanol or water demonstrates that the PEGDA resin with the NPS UV absorber can be made non-cytotoxic with a simple post-processing step. However, these wash times are only applicable for the specific cylindrical geometry of the tested substrates. We expect that wash times will increase for thicker prints and/or microfluidic channels in a device will need to be washed with flowing eluent.

Since the PEGDA resin with NPS UV absorber required post-print processing to combat cytotoxicity, and this is ultimately undesirable, another UV absorber was tested to ascertain if a resin could be made that required no post-print processing. Avobenzone is a UV absorber found in commercially available consumer products such as sunscreen. A PEGDA resin with this UV absorber was made at the same 1% Irgacure 819 photoinitiator concentration but with 0.38% avobenzone, which creates comparable absorption as 2% NPS because of its higher molar absorptivity. This resin formulation was tested for its cytotoxicity by the same direct contact method as the prior resin. As seen in Figure 5.2c, the avobenzone resin, with no post-processing, showed no signs of

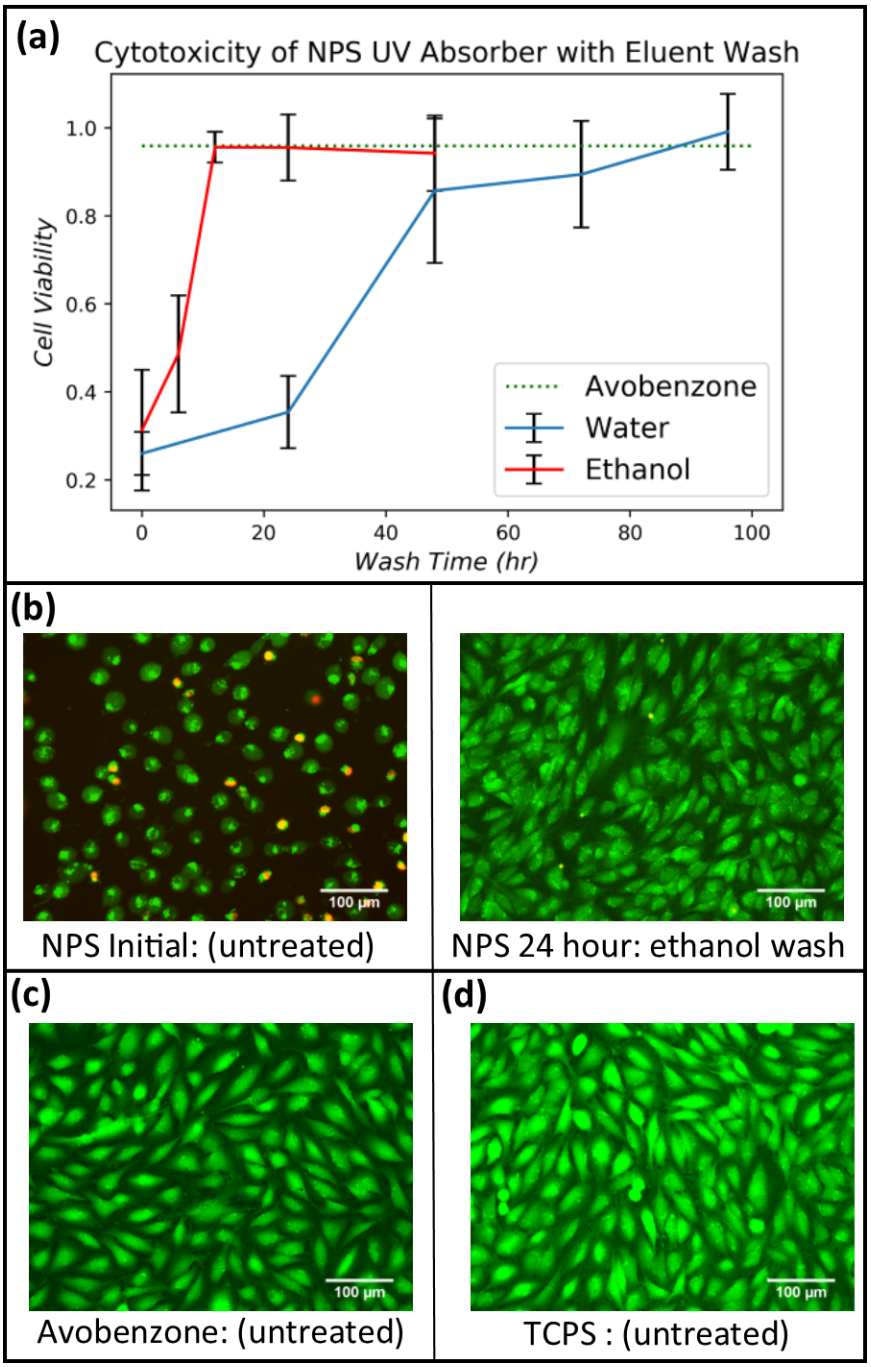

Figure 5.2: (a) Cytotoxicity of NPS UV Absorber with Eluent Wash: Data were normalized against a TCPS control seeded at the same density. A non-cytotoxic response, considered if greater than 70 %, was achieved using water after a 48 hour wash time, while if using ethanol only 12 hours was required. (b) Stained EA.hy926 cells undergoing cytotoxicity testing with resin containing NPS UV absorber. Both the initial untreated and 4-hour ethanol wash resins are shown. (c) Stained Ea.hy926 cells undergoing cytotoxicity testing with untreated resin containing avobenzone UV absorber. (d) stained EA.hy926 cells used as a control on TCPS.

cytotoxicity compared to a TCPS control, demonstrating that it is non-cytotoxic as-printed, and thus is a more attractive resin candidate for cell-based studies.

5.4 Cell Adherence

Note that the cytotoxicty testing does not give any information about cell adherence to 3D printed PEGDA. We therefore performed adherence testing on the PEGDA substrates with TCPS as a control to see how well anchoring proteins secreted from the cells adhered to the PEGDA material. After printing with either the NPS or avobenzone UV absorber, the substrates were sterilized and were placed in a sterile 12-well plate. Endothelial cells (EA.hy926) were then passaged into the wells of the 12-well plate such that the cells could attach and proliferate on the PEGDA material. The cells were viewed after a 24-hour exposure time and stained using a Calcein AM/EthD live/dead assay. Adherence was measured by image analysis using CellProfiler and calculating the fractional cell surface coverage of the adherent cells in comparison to the TCPS control which was passaged at the same cell density. Initial testing showed that the cells did not adhere well to the printed PEGDA material in its native state, even after previously discussed eluent treatments were performed to reduce the cytotoxicity of the materials. This is in harmony with various research groups reporting on the known overall protein-repellant nature of untreated PEG [81, 82]. It was apparent that further post-processing was needed to modify the PEG surface for protein adsorption and cell adherence on the PEGDA substrates. It is worth noting that these surface modifications will need to significantly increase protein adsorption in order for cells to remain adhered during the shear stress experienced in microfluidic channel lumens. This and other cell stressors in microfluidic devices are well summarized by Varma and Voldman [83].

Several surface modifications were attempted to allow for adherence of proteins to the PEGDA surface including a topographical modification and oxygen plasma treatment. Topographical modification and micropatterning has been shown to be effective in helping cells that adhere weakly to PEG have access to increased surface area and thus have a higher chance of adhering to the surface [81]. A simple topographical modification of small parallel channels (width: 20 μm, depth:10 μm, spacing: 20 μm) was attempted with little improvement over the unmodified surface.

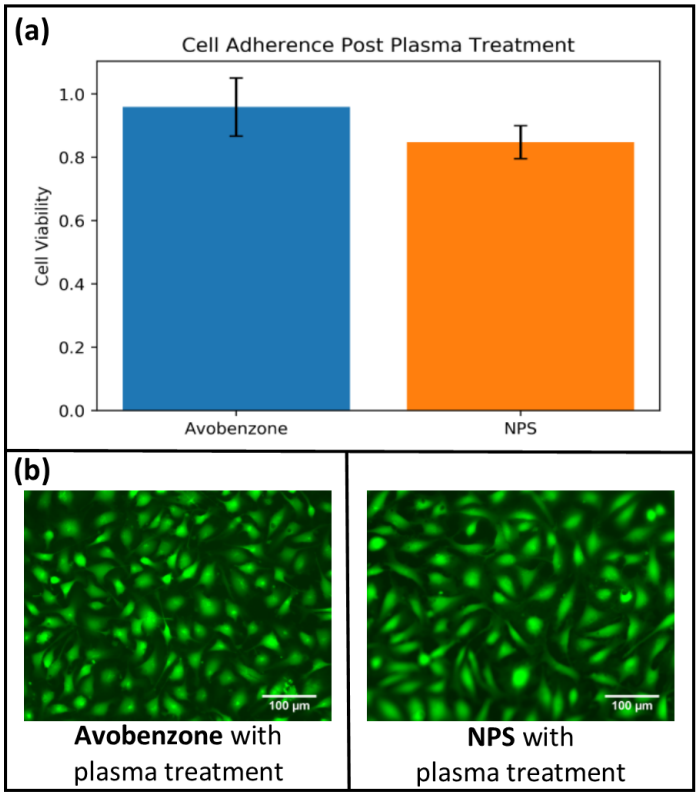

Figure 5.3: (a) Adherence of EA.hy926 cells to PEGDA test materials with different UV absorbers. Data are shown as the fractional surface coverage of the cells normalized to a TCPS control. These data suggest that after treatment with plasma, the materials allow the adherence of cellular proteins at a level similar to TCPS. (b) Image of adhered and stained EA.hy926 cells after plasma treatment on avobenzone and NPS resins.

Oxygen plasma treatment has also been shown to increase cellular adherence on PEGDA [14]. For this application, plasma treatment was chosen as a simple surface modification to allow for the attachment of cellular proteins. Another surface modification includes the addition of membrane proteins to the PEG and may be useful in later work if additional cellular adherence is needed [84]. For the plasma treatment, a Harrick Plasma Cleaner (Model PDC-32G) was used with standard lab atmosphere, not pure oxygen. The treatment was performed for 1-2 minutes. After plasma treatment, the substrates were sterilized and tested according to the procedure outlined above. Testing showed that the plasma treatment worked well to enhance cell attachment. This resulted in cell adherence at an average of 96% for the avobenzone, and 85% for the NPS UV absorber in comparison to a TCPS control as seen in Fig 5.3a. Therefore, a simple plasma treatment was sufficient to modify the PEGDA surface such that proteins were able to adhere to the surface

and allow for cell attachment. Further, the cell attachment to the avobenzone chips was statistically indistinguishable from the TCPS control, which bodes well for its further use in microfluidic cell culture.

5.5 Conclusion

In this study, a 3D printed resin consisting of PEGDA with 1% (w/w) Irgacure 819 with two different UV absorbers was tested for its cytotoxic properties with an endothelial cell line (EA.hy926). NPS, the first UV absorber tested, required a 12-hour post-printing ethanol wash to leech out cytotoxic contaminants in the material and afterward did not induce a cytotoxic cellular response when tested using the direct contact method outlined in ISO 10993-5. Avobenzone, the second UV absorber tested, did not require any post-print processing for cell compatibility.

Cell adherence was also tested for each PGEDA resin containing the different UV absorbers. Results showed that with a plasma treatment, both the NPS and avobenzone containing resins could support cell adhesion and in particular, the avobenzone containing resin was indistinguishable from TCPS controls. These tests show that 3D printed microfluidic devices can, with a few simple post-printing steps, be nontoxic to cells and allow for good cell adhesion in preparation for use in Lab-on-a-Chip applications.

CHAPTER 6. CONCLUSIONS AND FUTURE WORK

6.1 Conclusions

This thesis details how a bioprinting system was developed with four main conclusions. First, it was shown that a bioprinting system could be developed cheapy ($1000) from a commercially available 3D printer. Custom modifications can be made to suit the needs of researchers and the ever changing needs of bioprinting. Second, a collagen-based dECM bioink was developed that can provide a cheap and modifiable bioink for researchers to start from in developing bioink for tissue engineering applications. Third, a procedure for optimizing bioprinting parameters was developed using open-source software and a Raspberry Pi camera feedback system. Lastly, procedures were developed to make two resins with different UV absorbers, that are compatible with cells and able to be used in Lab-on-a-Chip applications.

6.2 Future Work

To continue this work, one of the next necessary steps will be to test the cytotoxicity and ability of the dECM bioink to allow for cell proliferation. The bioink will need to be reliably sterilized and tested with cells to see how they grow and if additional modifications need to be made. Following these cell tests, the printing of a vascular network would be an important benchmark. Channels of various diameter could be printed parallel to each other and with vascular promoting cells inlaid, such as smooth muscle cells or fibroblasts, and growth factors like VEGF, a vascular network could be made and tested to optimize the many variables that will come into play. The development of a vascular network will allow for the true testing of 3D cell culture and possibly aid in the progression towards a true artificial tissue.

Another avenue of future work involves the modeling of the bioprinting process. This could consist of the modeling of the bioink being extruded into the substrate and the subsequent

diffusion of the bioink before cross-linking. The slicing of a desired CAD model could then be optimized and slicing parameters modified that would allow for the modeled extrusion of the bioink to produce the desired structure. This would truly optimize the resolution of bioprinters and allow researchers to see where the limit of resolution lies.

REFERENCES

[1] R. Langer and J. Vacanti, "Advances in tissue engineering," *J Pediatr Surg*, vol. 51, no. 1, pp. 8–12, 2016. 1

[2] A. I. Smits, V. Bonito, and M. Stoddart, "In situ tissue engineering: Seducing the body to regenerate," *Tissue Eng Part A*, vol. 22, no. 17-18, pp. 1061–2, 2016. 1

[3] T. J. Hinton, A. Hudson, K. Pusch, A. Lee, and A. W. Feinberg, "3d printing pdms elastomer in a hydrophilic support bath via freeform reversible embedding," *Acs Biomaterials Science Engineering*, vol. 2, no. 10, pp. 1781–1786, 2016. 3, 16

[4] T. J. Hinton, Q. Jallerat, R. N. Palchesko, J. H. Park, M. S. Grodzicki, H.-J. Shue, M. H. Ramadan, A. R. Hudson, and A. W. Feinberg, "Three-dimensional printing of complex biological structures by freeform reversible embedding of suspended hydrogels," *Science Advances*, vol. 1, no. 9, p. e1500758, 2015. 3, 16, 17, 22

[5] C. J. Ferris, K. G. Gilmore, G. G. Wallace, and M. In het Panhuis, "Biofabrication: an overview of the approaches used for printing of living cells," *Appl Microbiol Biotechnol*, vol. 97, no. 10, pp. 4243–58, 2013. 6

[6] L. Elomaa and Y. P. Yang, "Additive manufacturing of vascular grafts and vascularized tissue constructs," *Tissue Eng Part B Rev*, vol. 23, no. 5, pp. 436–450, 2017. 6

[7] C. Mandrycky, Z. Wang, K. Kim, and D. H. Kim, "3d bioprinting for engineering complex tissues," *Biotechnol Adv*, vol. 34, no. 4, pp. 422–34, 2016. 6

[8] T. J. Hinton, A. Lee, and A. W. Feinberg, "3d bioprinting from the micrometer to millimeter length scales: Size does matter," *Current Opinion in Biomedical Engineering*, vol. 1, pp. 31–37, 2017. 6

[9] M. K. Wodarczyk-Biegun and A. del Campo, "3d bioprinting of structural proteins," *Biomaterials*, vol. 134, pp. 180–201, 2017. 6, 15

[10] C. M. Ho, S. H. Ng, K. H. Li, and Y. J. Yoon, "3d printed microfluidics for biological applications," *Lab Chip*, vol. 15, no. 18, pp. 3627–37, 2015. 6

[11] W. Zhang and S. Chen, "Femtosecond laser nanofabrication of hydrogel biomaterial," *MRS Bulletin*, vol. 36, no. 12, pp. 1028–1033, 2011. 6

[12] V. B. Morris, S. Nimbalkar, M. Younesi, P. McClellan, and O. Akkus, "Mechanical properties, cytocompatibility and manufacturability of chitosan:pegda hybrid-gel scaffolds by stereolithography," *Ann Biomed Eng*, vol. 45, no. 1, pp. 286–296, 2017. 6

[13] H. Gong, B. P. Bickham, A. T. Woolley, and G. P. Nordin, "Custom 3d printer and resin for 18 mum x 20 mum microfluidic flow channels," *Lab Chip*, vol. 17, no. 17, pp. 2899–2909, 2017. 6, 56, 57, 58

[14] A. Urrios, C. Parra-Cabrera, N. Bhattacharjee, A. M. Gonzalez-Suarez, L. G. Rigat-Brugarolas, U. Nallapatti, J. Samitier, C. A. DeForest, F. Posas, J. L. Garcia-Cordero, and A. Folch, "3d-printing of transparent bio-microfluidic devices in peg-da," *Lab Chip*, vol. 16, no. 12, pp. 2287–94, 2016. 6, 62

[15] B. Webb and B. J. Doyle, "Parameter optimization for 3d bioprinting of hydrogels," *Bioprinting*, vol. 8, pp. 8–12, 2017. 7, 36

[16] H. W. Kang, S. J. Lee, I. K. Ko, C. Kengla, J. J. Yoo, and A. Atala, "A 3d bioprinting system to produce human-scale tissue constructs with structural integrity," *Nat Biotechnol*, vol. 34, no. 3, pp. 312–9, 2016. 7

[17] D. B. Kolesky, K. A. Homan, M. A. Skylar-Scott, and J. A. Lewis, "Three-dimensional bioprinting of thick vascularized tissues," *Proc Natl Acad Sci U S A*, vol. 113, no. 12, pp. 3179–84, 2016. 7

[18] T. Pan, W. Song, X. Cao, and Y. Wang, "3d bioplotting of gelatin/alginate scaffolds for tissue engineering: Influence of crosslinking degree and pore architecture on physicochemical properties," *Journal of Materials Science Technology*, vol. 32, no. 9, pp. 889–900, 2016. 15

[19] B. Bagley, "Collagen bioinks for 3d bioprinting," *Tissue Engineering Part A*, vol. 23, pp. S57–S57, 2017. 15

[20] Y. Luo, G. Luo, M. Gelinsky, P. Huang, and C. Ruan, "3d bioprinting scaffold using alginate/polyvinyl alcohol bioinks," *Materials Letters*, vol. 189, pp. 295–298, 2017. 15

[21] H. Stratesteffen, M. Koepf, F. Kreimendahl, A. Blaeser, S. Jockenhoevel, and H. Fischer, "Gelma-collagen blends enable drop-on-demand 3d printablility and promote angiogenesis," *Biofabrication*, vol. 9, no. 4, 2017. 15

[22] X. Yang, Z. Lu, H. Wu, W. Li, L. Zheng, and J. Zhao, "Collagen-alginate as bioink for three-dimensional (3d) cell printing based cartilage tissue engineering," *Materials Science Engineering C-Materials for Biological Applications*, vol. 83, pp. 195–201, 2018. 15

[23] F. Pati, J. Jang, D. H. Ha, S. Won Kim, J. W. Rhie, J. H. Shim, D. H. Kim, and D. W. Cho, "Printing three-dimensional tissue analogues with decellularized extracellular matrix bioink," *Nat Commun*, vol. 5, p. 3935, 2014. 15, 25

[24] L. T. Saldin, M. C. Cramer, S. S. Velankar, L. J. White, and S. F. Badylak, "Extracellular matrix hydrogels from decellularized tissues: Structure and function," *Acta Biomater*, vol. 49, pp. 1–15, 2017. 15, 25

[25] C. Norotte, F. S. Marga, L. E. Niklason, and G. Forgacs, "Scaffold-free vascular tissue engineering using bioprinting," *Biomaterials*, vol. 30, no. 30, pp. 5910–7, 2009. 16

[26] E. A. Bulanova, E. V. Koudan, J. Degosserie, C. Heymans, F. D. A. S. Pereira, V. A. Parfenov, Y. Sun, Q. Wang, S. A. Akhmedova, I. K. Sviridova, N. S. Sergeeva, G. A. Frank, Y. D. Khesuani, C. E. Pierreux, and V. A. Mironov, "Bioprinting of a functional vascularized mouse thyroid gland construct," *Biofabrication*, vol. 9, no. 3, 2017. 16

[27] L. Ouyang, C. B. Highley, W. Sun, and J. A. Burdick, "A generalizable strategy for the 3d bioprinting of hydrogels from nonviscous photo-crosslinkable inks," *Adv Mater*, vol. 29, no. 8, 2017. 16

[28] K. Zhang, Q. Fu, J. Yoo, X. Chen, P. Chandra, X. Mo, L. Song, A. Atala, and W. Zhao, "3d bioprinting of urethra with pcl/plcl blend and dual autologous cells in fibrin hydrogel: An in vitro evaluation of biomimetic mechanical property and cell growth environment," *Acta Biomater*, vol. 50, pp. 154–164, 2017. 16

[29] K. Y. Lee and D. J. Mooney, "Alginate: properties and biomedical applications," *Prog Polym Sci*, vol. 37, no. 1, pp. 106–126, 2012. 21, 33

[30] J. Park, S. J. Lee, S. Chung, J. H. Lee, W. D. Kim, J. Y. Lee, and S. A. Park, "Cell-laden 3d bioprinting hydrogel matrix depending on different compositions for soft tissue engineering: Characterization and evaluation," *Mater Sci Eng C Mater Biol Appl*, vol. 71, pp. 678–684, 2017. 22

[31] T. Gao, G. J. Gillispie, J. S. Copus, A. K. Pr, Y. J. Seol, A. Atala, J. J. Yoo, and S. J. Lee, "Optimization of gelatin-alginate composite bioink printability using rheological parameters: a systematic approach," *Biofabrication*, vol. 10, no. 3, p. 034106, 2018. 22

[32] T. Andersen, P. Auk-Emblem, and M. Dornish, "3d cell culture in alginate hydrogels," *Microarrays (Basel)*, vol. 4, no. 2, pp. 133–61, 2015. 22

[33] S. T. Bendtsen, S. P. Quinnell, and M. Wei, "Development of a novel alginate-polyvinyl alcohol-hydroxyapatite hydrogel for 3d bioprinting bone tissue engineered scaffolds," *J Biomed Mater Res A*, vol. 105, no. 5, pp. 1457–1468, 2017. 22

[34] G. Lai, Y. Li, and G. Li, "Effect of concentration and temperature on the rheological behavior of collagen solution," *Int J Biol Macromol*, vol. 42, no. 3, pp. 285–91, 2008. 24

[35] A. Sionkowska, J. Skopinska-Wisniewska, M. Gawron, J. Kozlowska, and A. Planecka, "Chemical and thermal cross-linking of collagen and elastin hydrolysates," *Int J Biol Macromol*, vol. 47, no. 4, pp. 570–7, 2010. 24

[36] A. Isaacson, S. Swioklo, and C. J. Connon, "3d bioprinting of a corneal stroma equivalent," *Exp Eye Res*, 2018. 24

[37] V. K. Lee, A. M. Lanzi, N. Haygan, S. S. Yoo, P. A. Vincent, and G. Dai, "Generation of multi-scale vascular network system within 3d hydrogel using 3d bio-printing technology," *Cell Mol Bioeng*, vol. 7, no. 3, pp. 460–472, 2014. 24, 31

[38] B. D. MacNeill, I. Pomerantseva, H. C. Lowe, S. N. Oesterle, and J. P. Vacanti, "Toward a new blood vessel," *Vasc Med*, vol. 7, no. 3, pp. 241–6, 2002. 24

[39] R. Kaye, T. Goldstein, D. A. Grande, D. Zeltsman, and L. P. Smith, "A 3-dimensional bioprinted tracheal segment implant pilot study: Rabbit tracheal resection with graft implantation," *Int J Pediatr Otorhinolaryngol*, vol. 117, pp. 175–178, 2019. 24

[40] M. Izadifar, D. Chapman, P. Babyn, X. Chen, and M. E. Kelly, "Uv-assisted 3d bioprinting of nanoreinforced hybrid cardiac patch for myocardial tissue engineering," *Tissue Eng Part C Methods*, vol. 24, no. 2, pp. 74–88, 2018. 24

[41] X. Wang, M. S. Ali, and C. M. R. Lacerda, "A three-dimensional collagen-elastin scaffold for heart valve tissue engineering," *Bioengineering (Basel)*, vol. 5, no. 3, 2018. 24

[42] A. Mazzocchi, M. Devarasetty, R. Huntwork, S. Soker, and A. Skardal, "Optimization of collagen type i-hyaluronan hybrid bioink for 3d bioprinted liver microenvironments," *Biofabrication*, vol. 11, no. 1, p. 015003, 2018. 24

[43] N. Momtahan, S. Sukavaneshvar, B. L. Roeder, and A. D. Cook, "Strategies and processes to decellularize and recellularize hearts to generate functional organs and reduce the risk of thrombosis," *Tissue Eng Part B Rev*, vol. 21, no. 1, pp. 115–32, 2015. 25, 26, 29

[44] M. T. Wolf, K. A. Daly, E. P. Brennan-Pierce, S. A. Johnson, C. A. Carruthers, A. D'Amore, S. P. Nagarkar, S. S. Velankar, and S. F. Badylak, "A hydrogel derived from decellularized dermal extracellular matrix," *Biomaterials*, vol. 33, no. 29, pp. 7028–38, 2012. 25

[45] S. F. Badylak, D. Taylor, and K. Uygun, "Whole-organ tissue engineering: decellularization and recellularization of three-dimensional matrix scaffolds," *Annu Rev Biomed Eng*, vol. 13, pp. 27–53, 2011. 25

[46] T. D. Johnson, S. Y. Lin, and K. L. Christman, "Tailoring material properties of a nanofibrous extracellular matrix derived hydrogel," *Nanotechnology*, vol. 22, no. 49, p. 494015, 2011. 25

[47] S. Seif-Naraghi, J. Singelyn, J. Dequach, P. Schup-Magoffin, and K. Christman, "Fabrication of biologically derived injectable materials for myocardial tissue engineering," *J Vis Exp*, no. 46, 2010. 25

[48] J. M. Singelyn, J. A. DeQuach, S. B. Seif-Naraghi, R. B. Littlefield, P. J. Schup-Magoffin, and K. L. Christman, "Naturally derived myocardial matrix as an injectable scaffold for cardiac tissue engineering," *Biomaterials*, vol. 30, no. 29, pp. 5409–16, 2009. 25

[49] J. M. Singelyn, P. Sundaramurthy, T. D. Johnson, P. J. Schup-Magoffin, D. P. Hu, D. M. Faulk, J. Wang, K. M. Mayle, K. Bartels, M. Salvatore, A. M. Kinsey, A. N. Demaria, N. Dib, and K. L. Christman, "Catheter-deliverable hydrogel derived from decellularized ventricular extracellular matrix increases endogenous cardiomyocytes and preserves cardiac function post-myocardial infarction," *J Am Coll Cardiol*, vol. 59, no. 8, pp. 751–63, 2012. 25

[50] J. L. Ungerleider, T. D. Johnson, N. Rao, and K. L. Christman, "Fabrication and characterization of injectable hydrogels derived from decellularized skeletal and cardiac muscle," *Methods*, vol. 84, pp. 53–9, 2015. 25

[51] R. M. Wang and K. L. Christman, "Decellularized myocardial matrix hydrogels: In basic research and preclinical studies," *Adv Drug Deliv Rev*, vol. 96, pp. 77–82, 2016. 25

[52] J. Jang, T. G. Kim, B. S. Kim, S. W. Kim, S. M. Kwon, and D. W. Cho, "Tailoring mechanical properties of decellularized extracellular matrix bioink by vitamin b2-induced photocrosslinking," *Acta Biomater*, vol. 33, pp. 88–95, 2016. 25

[53] B. S. Kim, Y. W. Kwon, J. S. Kong, G. T. Park, G. Gao, W. Han, M. B. Kim, H. Lee, J. H. Kim, and D. W. Cho, "3d cell printing of in vitro stabilized skin model and in vivo pre-vascularized skin patch using tissue-specific extracellular matrix bioink: A step towards advanced skin tissue engineering," *Biomaterials*, vol. 168, pp. 38–53, 2018. 25

[54] F. Pati, D. H. Ha, J. Jang, H. H. Han, J. W. Rhie, and D. W. Cho, "Biomimetic 3d tissue printing for soft tissue regeneration," *Biomaterials*, vol. 62, pp. 164–75, 2015. 25

[55] D. O. Freytes, J. Martin, S. S. Velankar, A. S. Lee, and S. F. Badylak, "Preparation and rheological characterization of a gel form of the porcine urinary bladder matrix," *Biomaterials*, vol. 29, no. 11, pp. 1630–7, 2008. 26

[56] Y. Fu, X. Fan, C. Tian, J. Luo, Y. Zhang, L. Deng, T. Qin, and Q. Lv, "Decellularization of porcine skeletal muscle extracellular matrix for the formulation of a matrix hydrogel: a preliminary study," *J Cell Mol Med*, vol. 20, no. 4, pp. 740–9, 2016. 26

[57] C. A. Pacak, A. A. MacKay, and D. B. Cowan, "An improved method for the preparation of type i collagen from skin," *J Vis Exp*, no. 83, p. e51011, 2014. 26

[58] C. A. Pacak, J. M. Powers, and D. B. Cowan, "Ultrarapid purification of collagen type i for tissue engineering applications," *Tissue Eng Part C Methods*, vol. 17, no. 9, pp. 879–85, 2011. 26

[59] F. Yu, C. Zong, S. Jin, J. Zheng, N. Chen, J. Huang, Y. Chen, F. Huang, Z. Yang, Y. Tang, and G. Ding, "Optimization of extraction conditions and characterization of pepsin-solubilised collagen from skin of giant croaker (nibea japonica)," *Mar Drugs*, vol. 16, no. 1, 2018. 26

[60] L. Gui and L. E. Niklason, "Vascular tissue engineering: Building perfusable vasculature for implantation," *Curr Opin Chem Eng*, vol. 3, pp. 68–74, 2014. 31

[61] G. R. Fercana, S. Yerneni, M. Billaud, J. C. Hill, P. VanRyzin, T. D. Richards, B. M. Sicari, S. A. Johnson, S. F. Badylak, P. G. Campbell, T. G. Gleason, and J. A. Phillippi, "Perivascular extracellular matrix hydrogels mimic native matrix microarchitecture and promote angiogenesis via basic fibroblast growth factor," *Biomaterials*, vol. 123, pp. 142–154, 2017. 31

[62] K. T. Morin and R. T. Tranquillo, "In vitro models of angiogenesis and vasculogenesis in fibrin gel," *Exp Cell Res*, vol. 319, no. 16, pp. 2409–17, 2013. 31

[63] P. de la Puente and D. Ludena, "Cell culture in autologous fibrin scaffolds for applications in tissue engineering," *Exp Cell Res*, vol. 322, no. 1, pp. 1–11, 2014. 34

[64] Y. Li, H. Meng, Y. Liu, and B. P. Lee, "Fibrin gel as an injectable biodegradable scaffold and cell carrier for tissue engineering," *ScientificWorldJournal*, vol. 2015, p. 685690, 2015. 34

[65] P. T. Smith, A. Basu, A. Saha, and A. Nelson, "Chemical modification and printability of shear-thinning hydrogel inks for direct-write 3d printing," *Polymer*, 2018. 36

[66] G. Zhong, M. Vaezi, P. Liu, L. Pan, and S. Yang, "Characterization approach on the extrusion process of bioceramics for the 3d printing of bone tissue engineering scaffolds," *Ceramics International*, vol. 43, no. 16, pp. 13860–13868, 2017. 36

[67] P. Ertl, D. Sticker, V. Charwat, C. Kasper, and G. Lepperdinger, "Lab-on-a-chip technologies for stem cell analysis," *Trends Biotechnol*, vol. 32, no. 5, pp. 245–53, 2014. 56

[68] J. H. Tsui, W. Lee, S. H. Pun, J. Kim, and D. H. Kim, "Microfluidics-assisted in vitro drug screening and carrier production," *Adv Drug Deliv Rev*, vol. 65, no. 11-12, pp. 1575–88, 2013. 56

[69] J. Wu, Q. Chen, W. Liu, Z. He, and J.-M. Lin, "Recent advances in microfluidic 3d cellular scaffolds for drug assays," *TrAC Trends in Analytical Chemistry*, vol. 87, pp. 19–31, 2017. 56

[70] J. Wu, Z. He, Q. Chen, and J.-M. Lin, "Biochemical analysis on microfluidic chips," *TrAC Trends in Analytical Chemistry*, vol. 80, pp. 213–231, 2016. 56

[71] X. T. Zheng, L. Yu, P. Li, H. Dong, Y. Wang, Y. Liu, and C. M. Li, "On-chip investigation of cell-drug interactions," *Adv Drug Deliv Rev*, vol. 65, no. 11-12, pp. 1556–74, 2013. 56

[72] Q.-C. Zhuang, R.-Z. Ning, Y. Ma, and J.-M. Lin, "Recent developments in microfluidic chip for in vitro cell-based research," *Chinese Journal of Analytical Chemistry*, vol. 44, no. 4, pp. 522–532, 2016. 56

[73] E. K. Parker, A. V. Nielsen, M. J. Beauchamp, H. M. Almughamsi, J. B. Nielsen, M. Sonker, H. Gong, G. P. Nordin, and A. T. Woolley, "3d printed microfluidic devices with immunoaffinity monoliths for extraction of preterm birth biomarkers," *Anal Bioanal Chem*, 2018. 56

[74] S. Halldorsson, E. Lucumi, R. Gomez-Sjoberg, and R. M. T. Fleming, "Advantages and challenges of microfluidic cell culture in polydimethylsiloxane devices," *Biosens Bioelectron*, vol. 63, pp. 218–231, 2015. 56

[75] D. Huh, D. C. Leslie, B. D. Matthews, J. P. Fraser, S. Jurek, G. A. Hamilton, K. S. Thorneloe, M. A. McAlexander, and D. E. Ingber, "A human disease model of drug toxicity-induced pulmonary edema in a lung-on-a-chip microdevice," *Sci Transl Med*, vol. 4, no. 159, p. 159ra147, 2012. 56

[76] H. C. Huang, Y. J. Chang, W. C. Chen, H. I. Harn, M. J. Tang, and C. C. Wu, "Enhancement of renal epithelial cell functions through microfluidic-based coculture with adipose-derived stem cells," *Tissue Eng Part A*, vol. 19, no. 17-18, pp. 2024–34, 2013. 56

[77] J. M. H. Samuel Zalipsky, *Introduction to Chemistry and Biological Applications of Poly(ethylene glycol)*, book section 1, pp. 1–13. Washington, DC: American Chemical Society, 1997. 57

[78] H. Gong, A. T. Woolley, and G. P. Nordin, "3d printed high density, reversible, chip-to-chip microfluidic interconnects," *Lab Chip*, vol. 18, no. 4, pp. 639–647, 2018. 57, 58

[79] H. Gong, A. T. Woolley, and G. P. Nordin, "3d printed selectable dilution mixer pumps," *Biomicrofluidics*, vol. 13, no. 1, p. 014106, 2019. 57, 58

[80] M. J. Beauchamp, H. Gong, A. T. Woolley, and G. P. Nordin, "3d printed microfluidic features using dose control in x, y, and z dimensions," *Micromachines (Basel)*, vol. 9, no. 7, 2018. 58

[81] M. D. Marga C. Lensen, Vera A. Schulte, *Cell Adhesion and Spreading on an Intrinsically Anti-Adhesive PEG Biomaterial*. IntechOpen, 2011. 61

[82] P. N. Nge, J. V. Pagaduan, M. Yu, and A. T. Woolley, "Microfluidic chips with reversed-phase monoliths for solid phase extraction and on-chip labeling," *J Chromatogr A*, vol. 1261, pp. 129–35, 2012. 61

[83] S. Varma and J. Voldman, "Caring for cells in microsystems: principles and practices of cell-safe device design and operation," *Lab Chip*, vol. 18, no. 22, pp. 3333–3352, 2018. 61

[84] D. Missirlis and J. P. Spatz, "Combined effects of peg hydrogel elasticity and cell-adhesive coating on fibroblast adhesion and persistent migration," *Biomacromolecules*, vol. 15, no. 1, pp. 195–205, 2014. 62